United States Patent [19]

Rabl

[11] **4,054,390**

[45] **Oct. 18, 1977**

[54] APPARATUS FOR INVESTIGATING FAST CHEMICAL REACTIONS BY OPTICAL DETECTION

[75] Inventor: **Carl-Roland Rabl,** Gottingen, Germany

[73] Assignee: **Max-Planck-Gesellschaft zur Foerderung der Wissenschaften e.V.,** Gottingen, Germany

[21] Appl. No.: **686,029**

[22] Filed: **May 13, 1976**

Related U.S. Application Data

[62] Division of Ser. No. 487,592, July 11, 1974, Pat. No. 3,972,627.

[30] **Foreign Application Priority Data**

Dec. 19, 1973 Germany 2363180

[51] **Int. Cl.**^{2} **G01N 21/24**

[52] **U.S. Cl.** **356/206;** 250/574; 250/239

[58] **Field of Search** 356/103, 104, 204, 206, 356/208, 244, 246; 250/239, 573, 574, 575

[56] **References Cited**

U.S. PATENT DOCUMENTS

2,673,935 3/1954 Waldhaver 250/239

OTHER PUBLICATIONS

Czerlinski; G., "Versatile Temperature Jump Apparatus for Following Chemical Relaxations," *The Review of Scientific Instruments,* vol. 33, No. 11, Nov. 1962, pp. 1154–1159.

Czerlinski; G., "Timed Signal Grounding Switch for Observation of Low Level Signals Following Large Transients," *The Review of Scientific Instruments,* vol. 39, No. 11, Nov. 1968, pp. 1730–1732.

Primary Examiner—John K. Corbin
Assistant Examiner—R. A. Rosenberger
Attorney, Agent, or Firm—Flynn & Frishauf

[57] ABSTRACT

An apparatus for investigating the course of fast chemical reactions, which are initiated in a liquid chemical system under investigation by an external perturbation, e.g. a steep temperature rise (temperature jump). The apparatus comprises first and second light paths conveying a probing light beam and a sense light beam, respectively, and an optical system of extremely high aperture which allows a wide variety of types of measurements, including absorption, fluorescence, fluorescence polarization, and the like with a high signal-to-noise ratio even if small sample concentrations are used.

3 Claims, 15 Drawing Figures

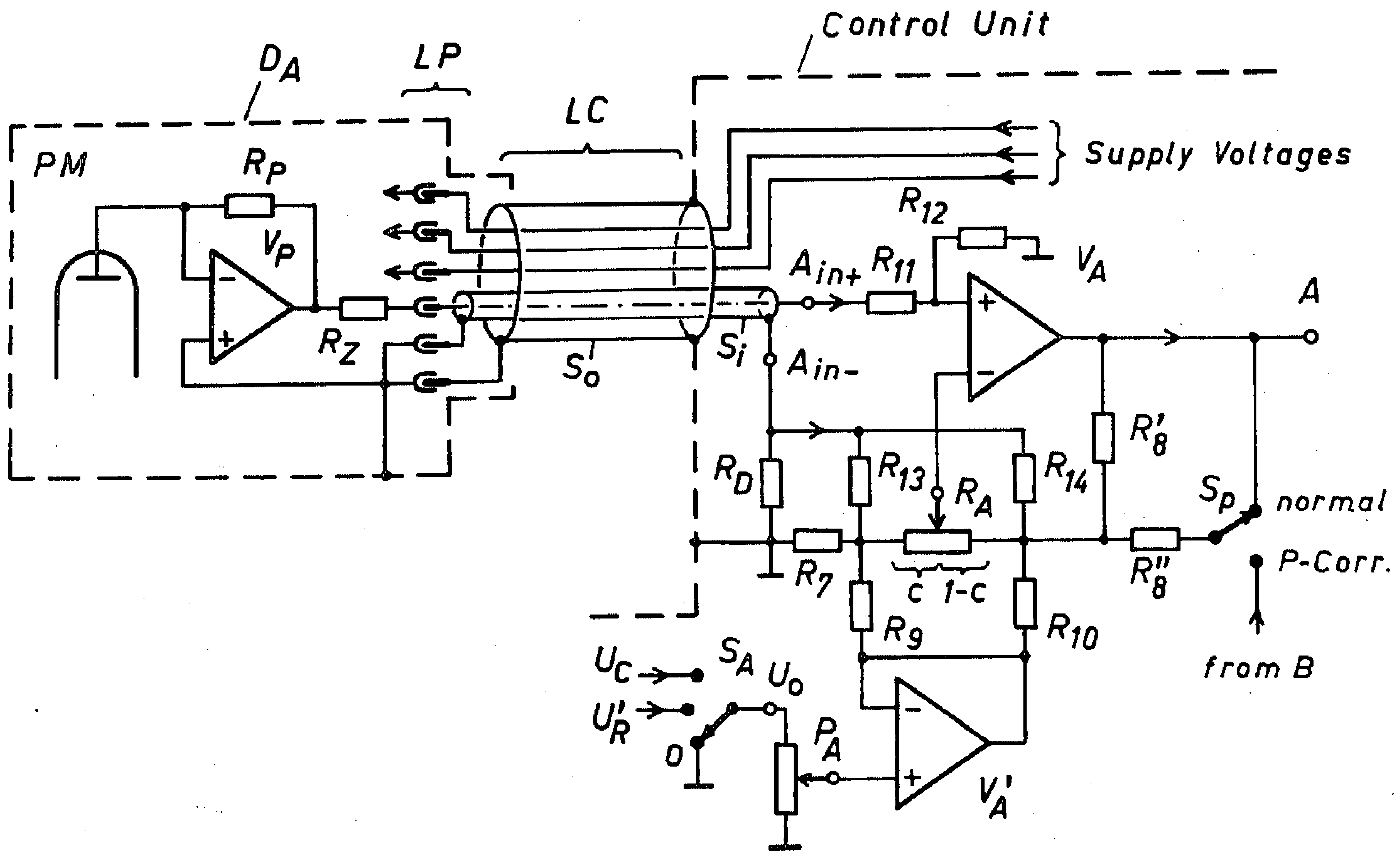

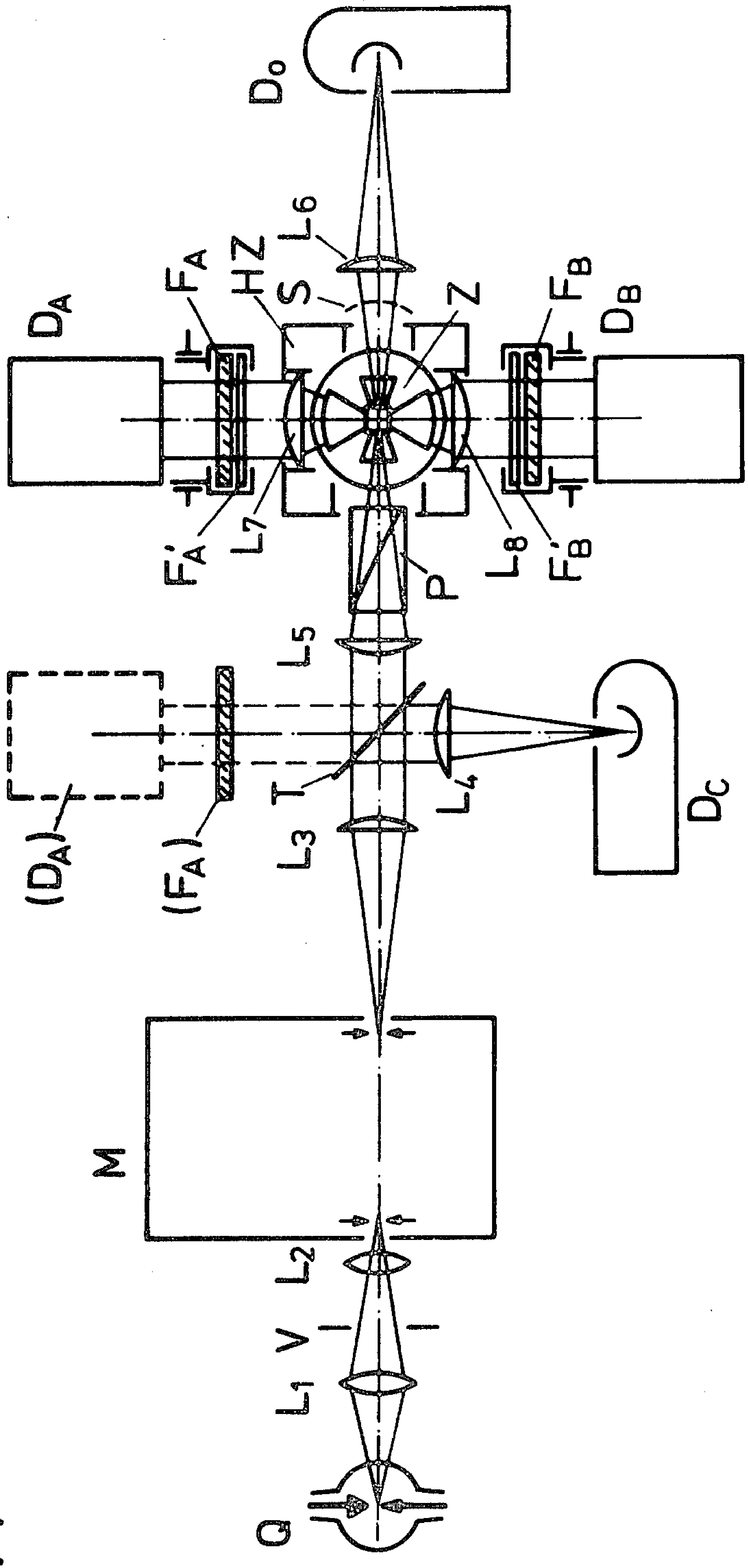

Fig. 1

Fig. 2. a)

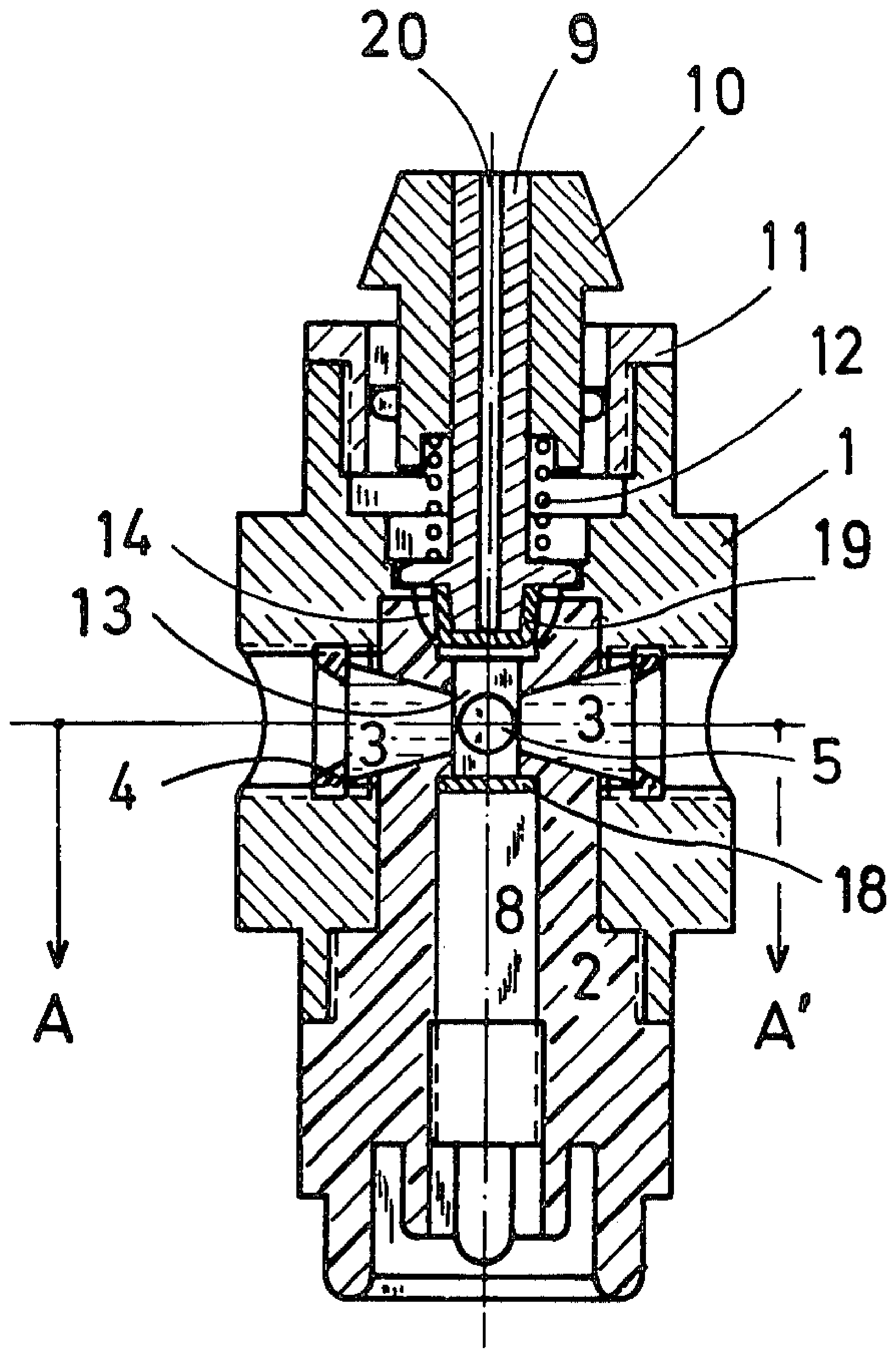

Fig. 2. b)

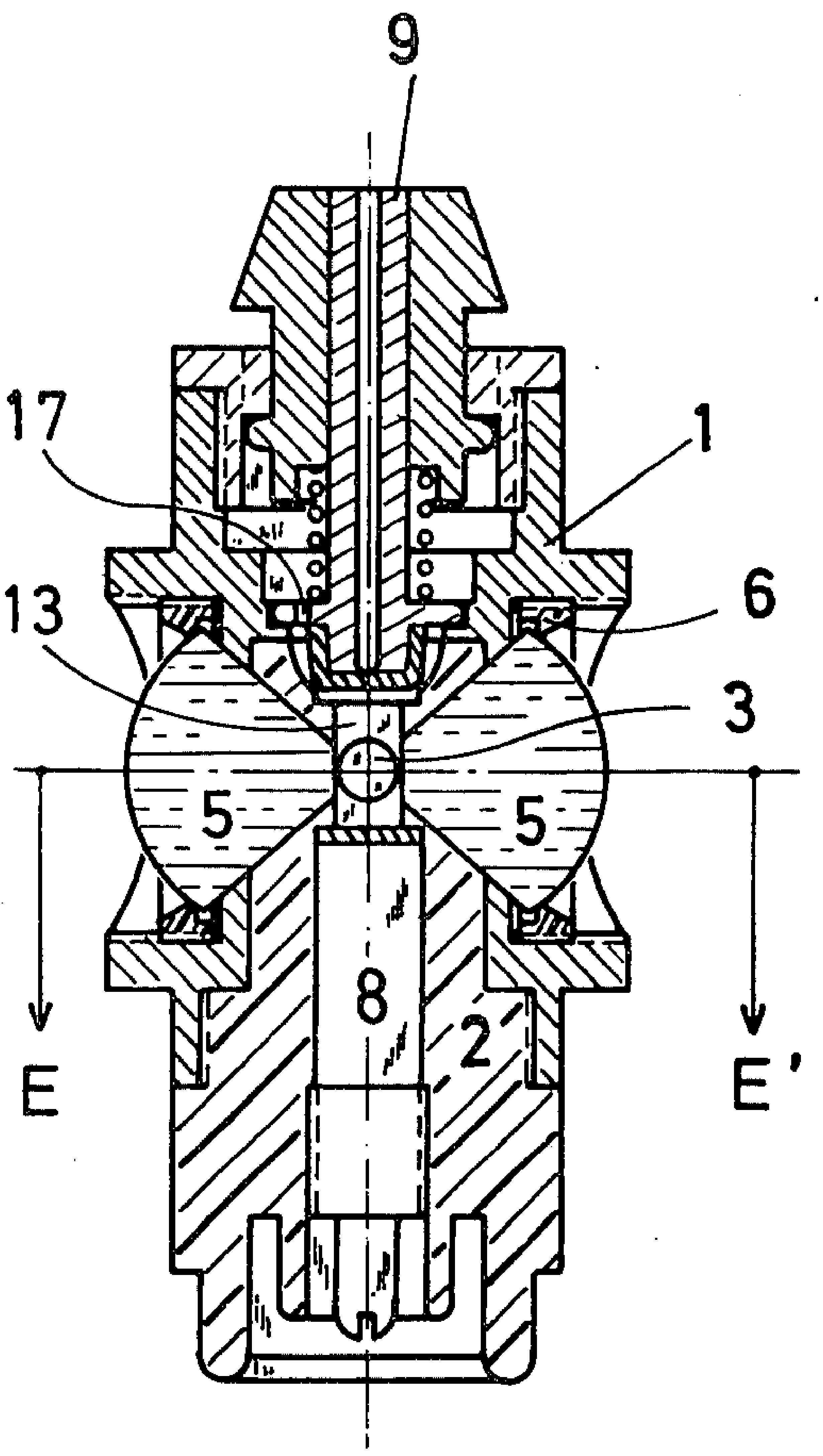

Fig. 2. c)

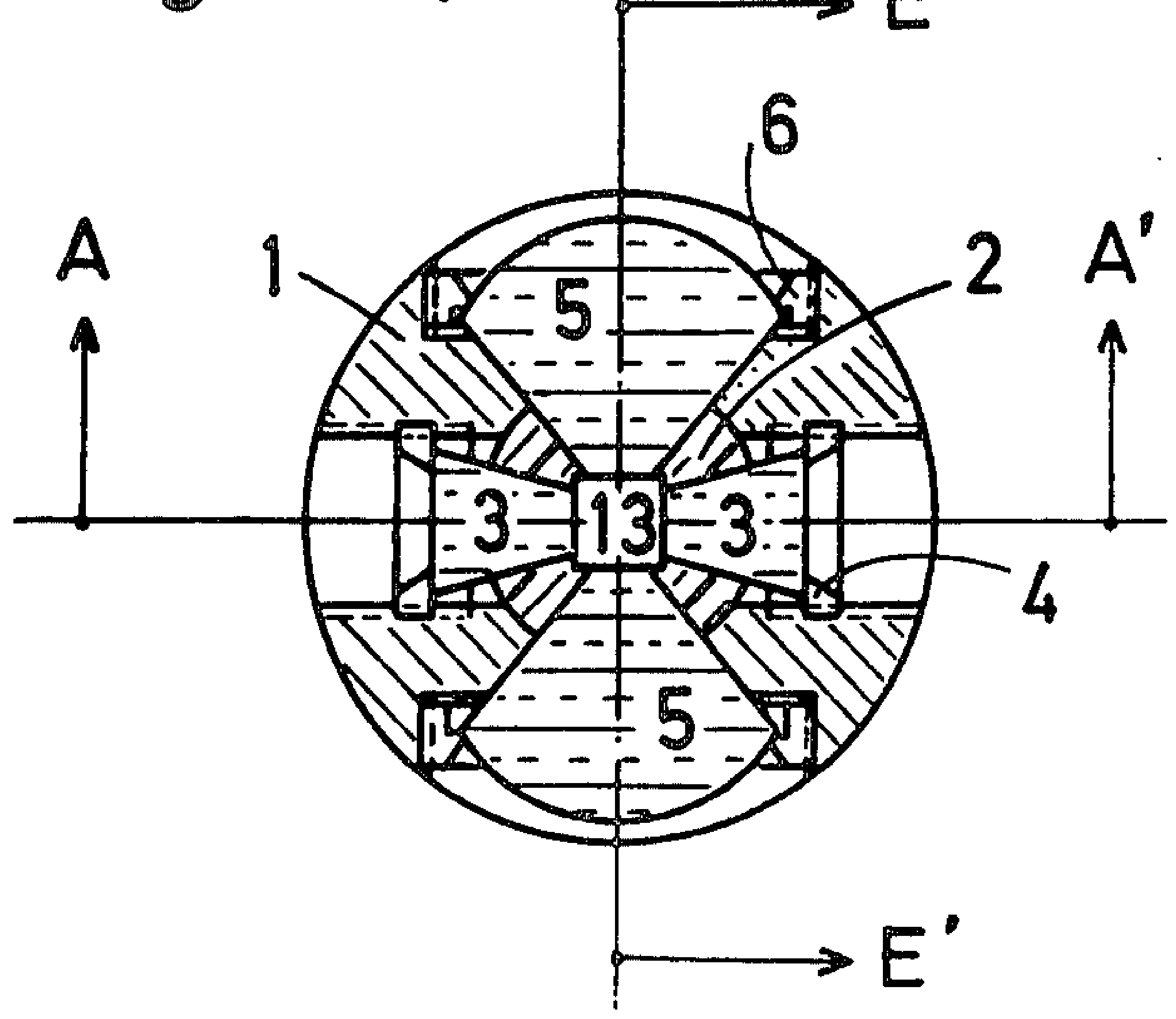

Fig. 2. d)

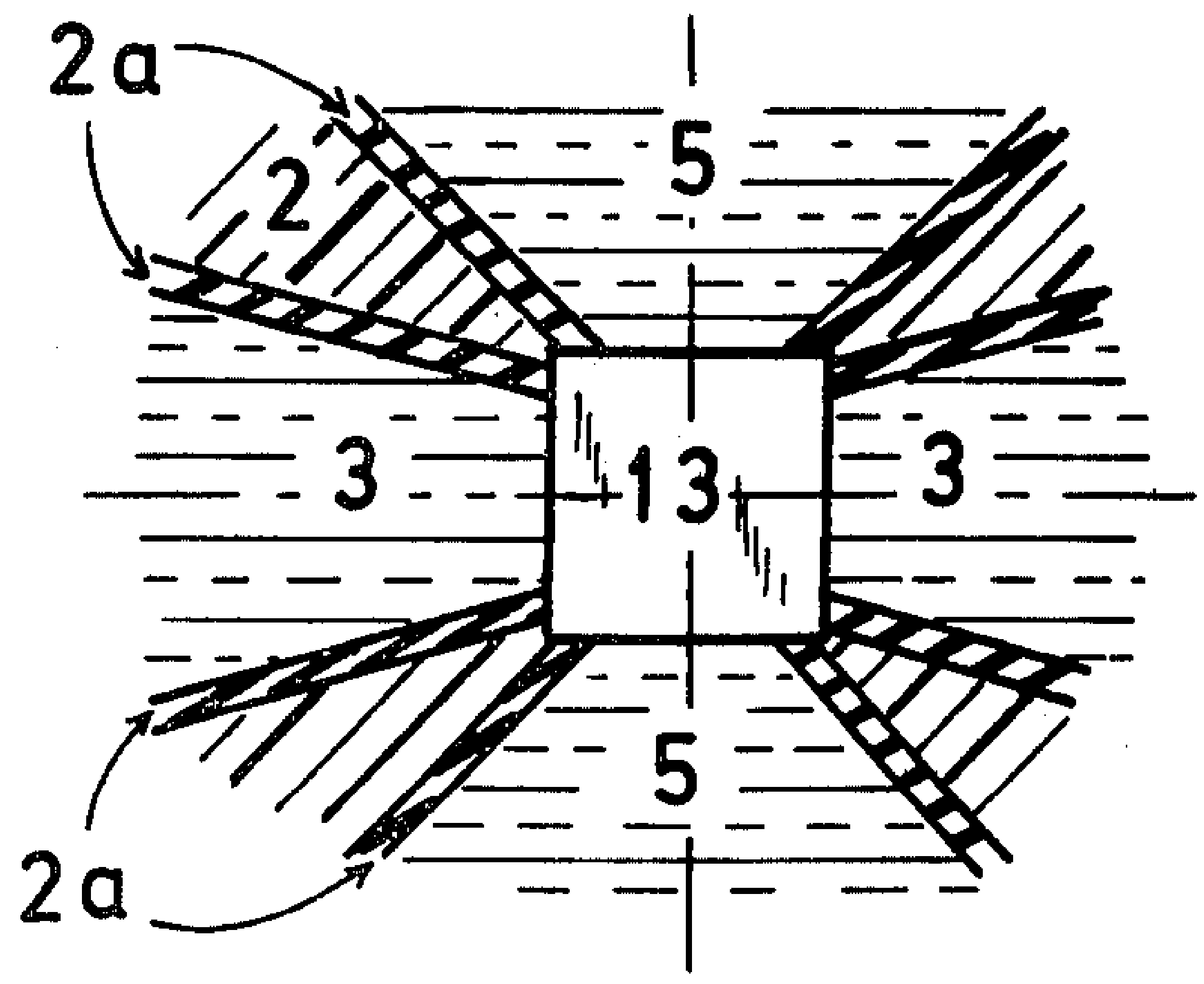

Fig. 2.e)

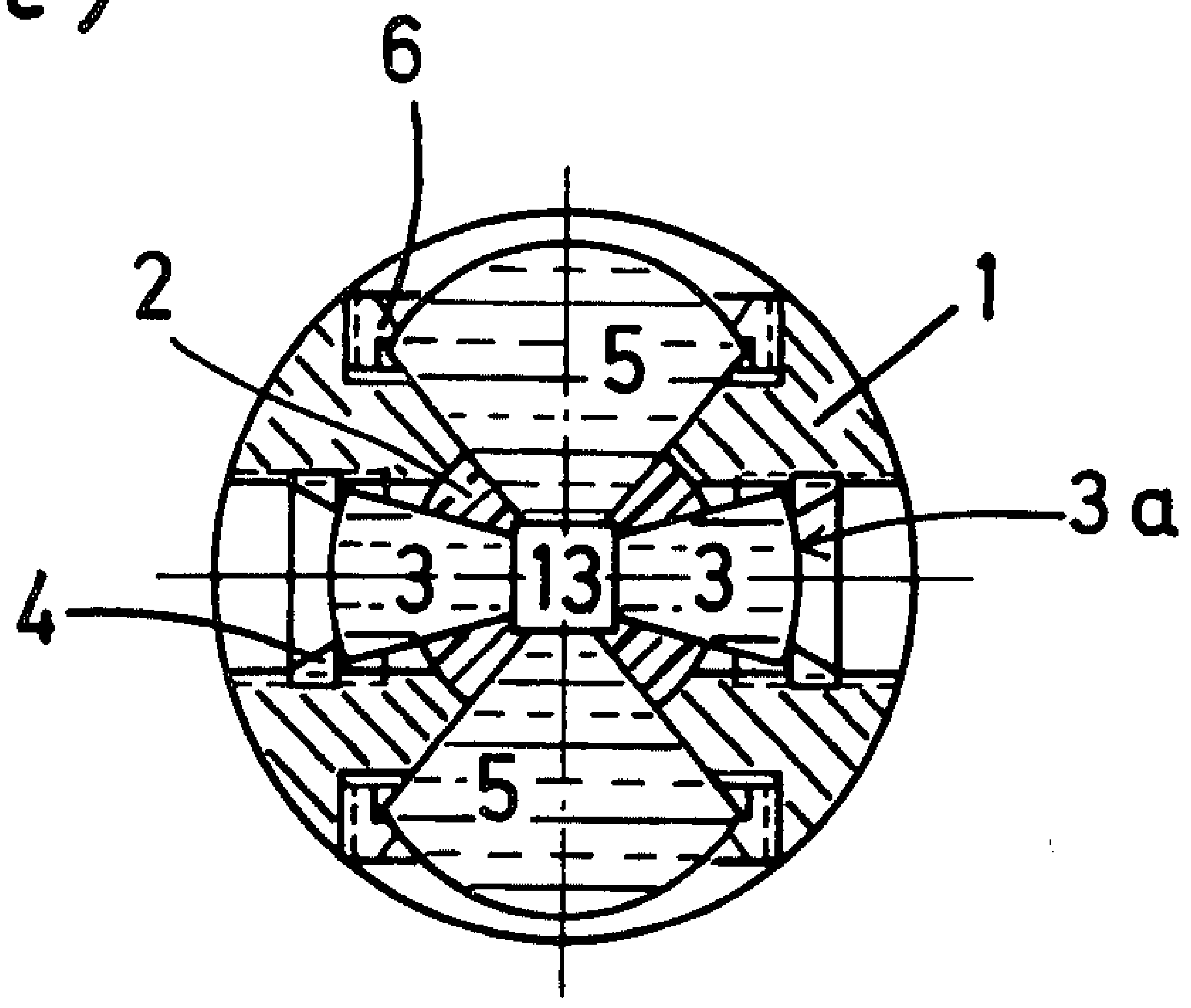

Fig. 2.f)

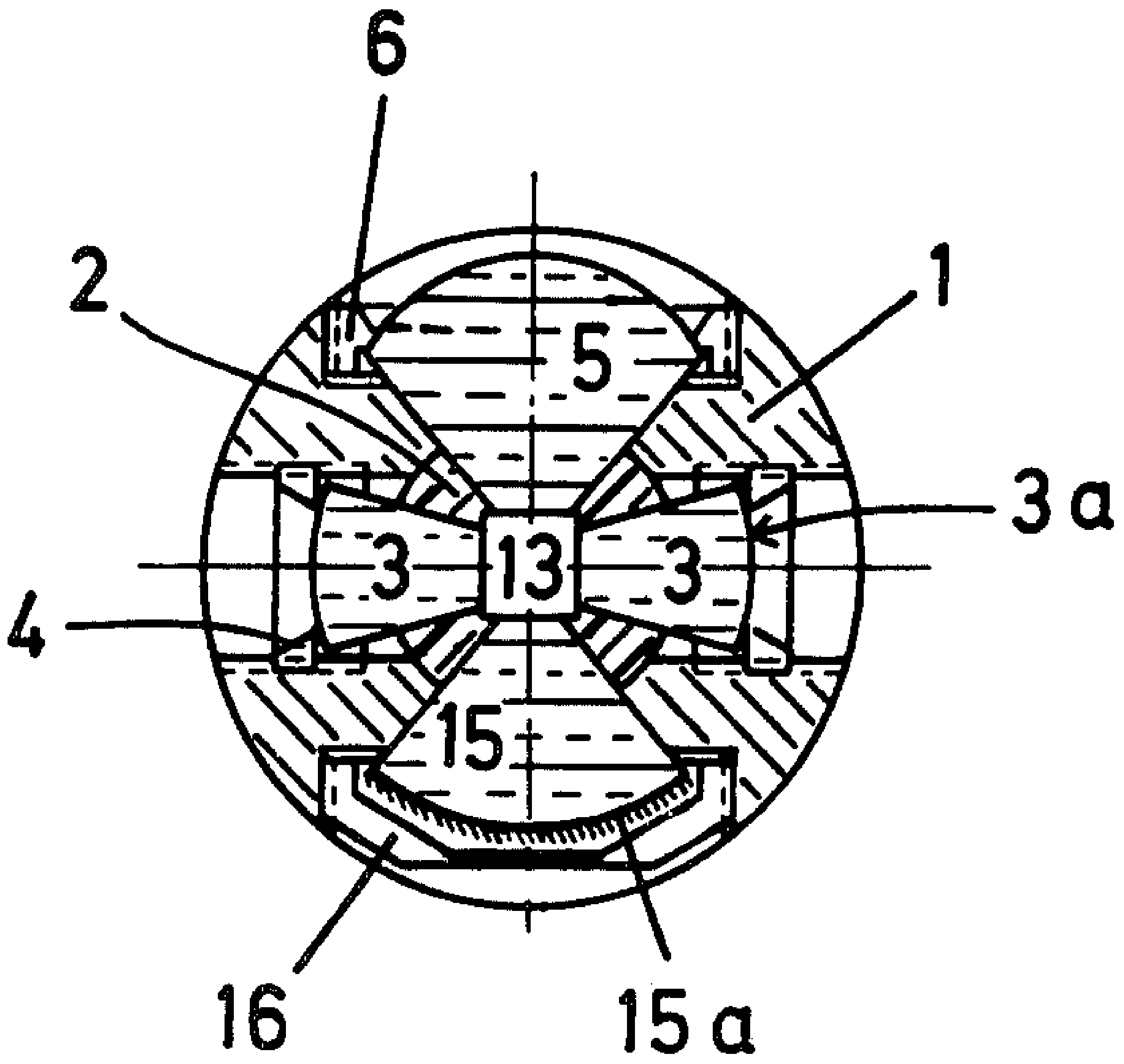

Fig. 3

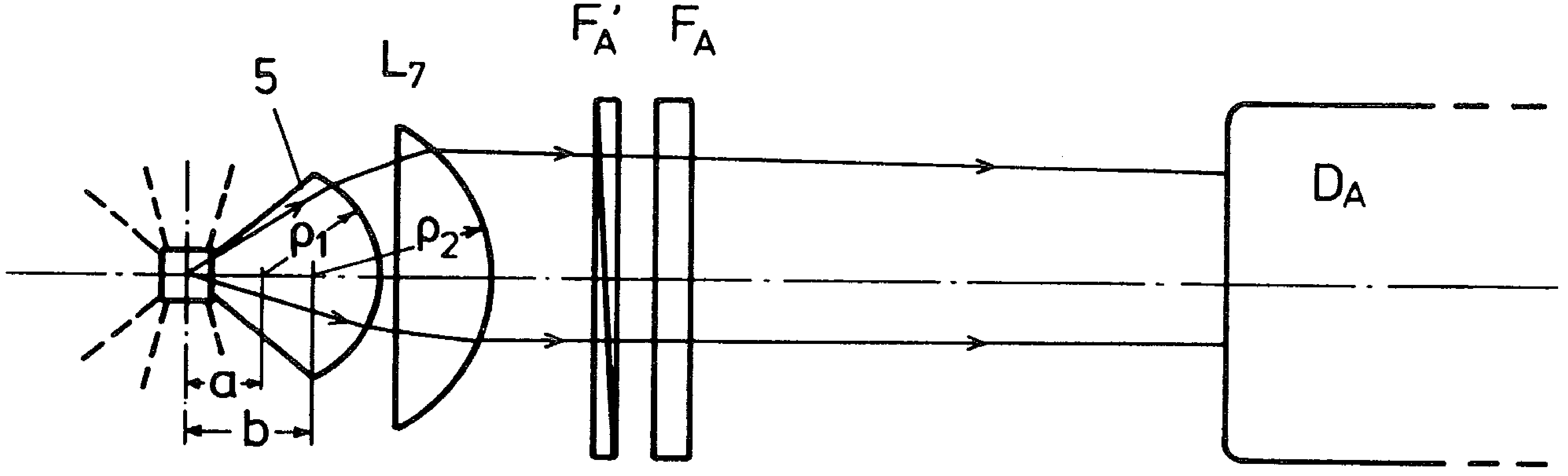

Fig. 4

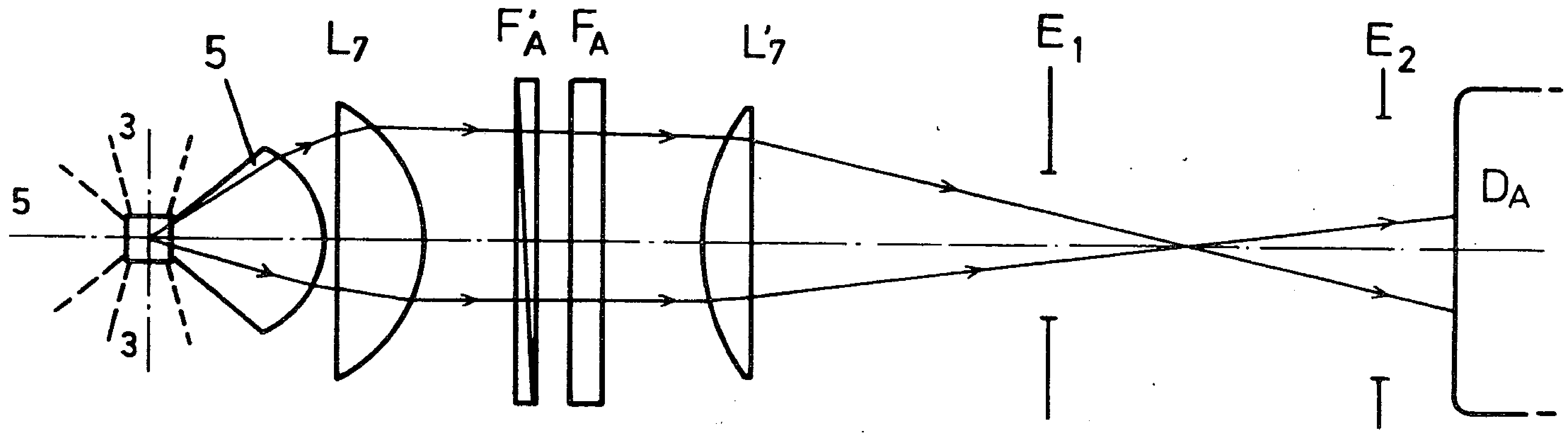

Fig. 5

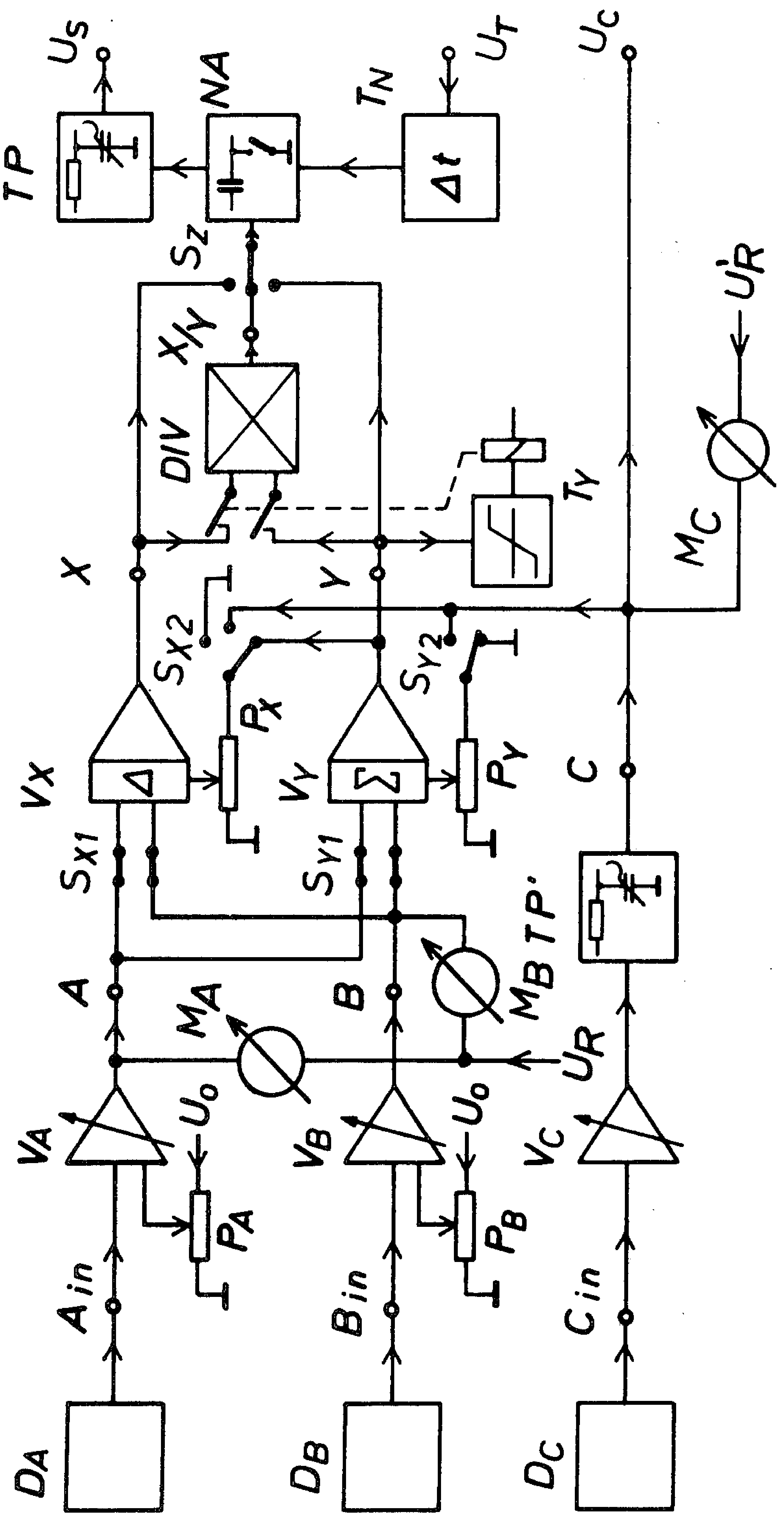
DA
DB
DC
Ain
Bin
Cin
PA
PB
VA
VB
VC
Uo
Uo
MA
MB
UR
A
B
TP'
C
Sx1
Sy1
Vx
Vy
Px
Py
Sx2
Sy2
X
Y
Ty
Mc
U'R
DIV
X/Y
Sz
TP
NA
TN
Δt
Us
UT
Uc

Fig.6

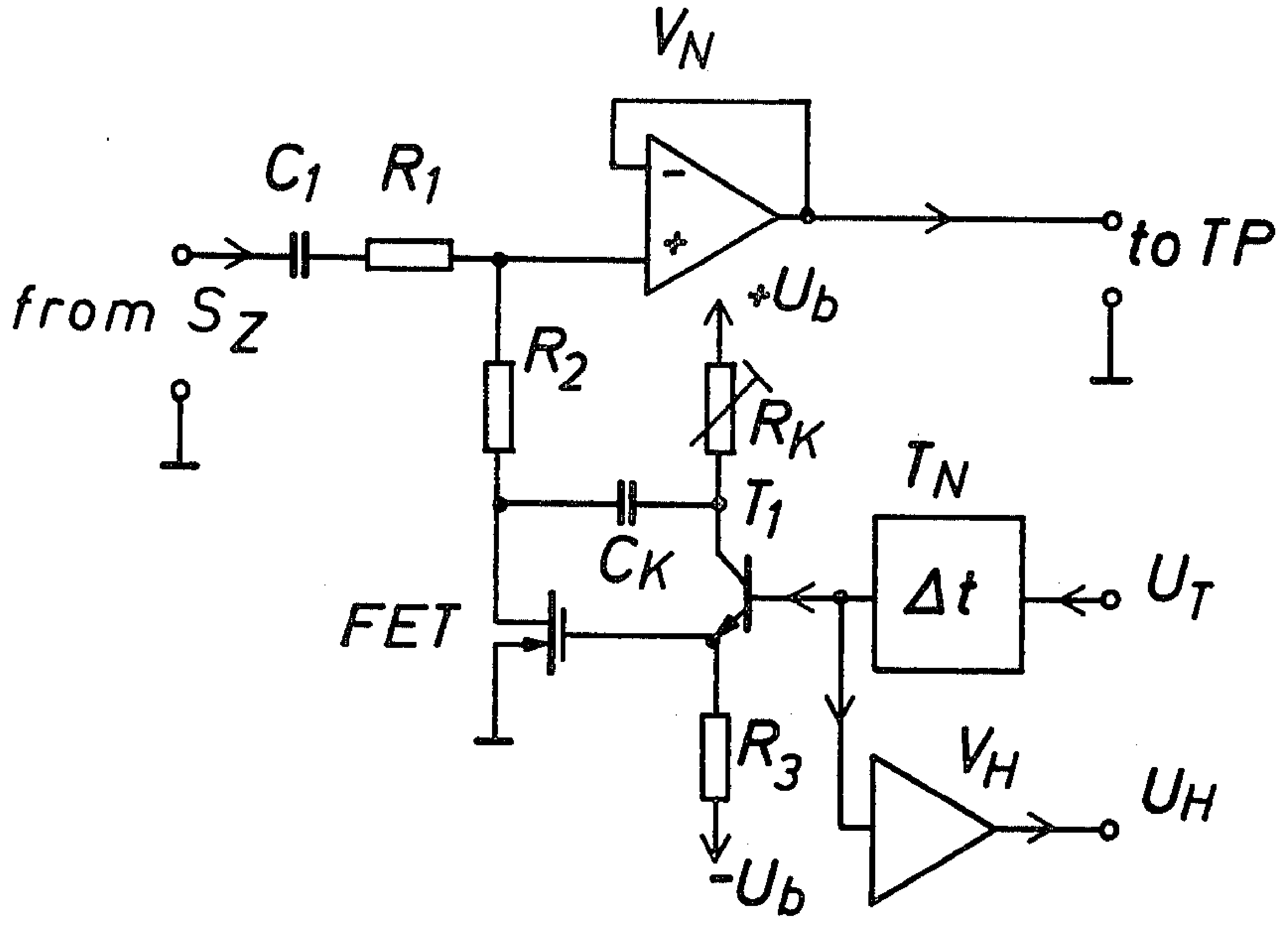

V_N
C_1
R_1
from S_Z
to TP
$+U_b$
R_2
R_K
T_N
T_1
C_K
FET
Δt
U_T
R_3
V_H
U_H
$-U_b$

Fig.7

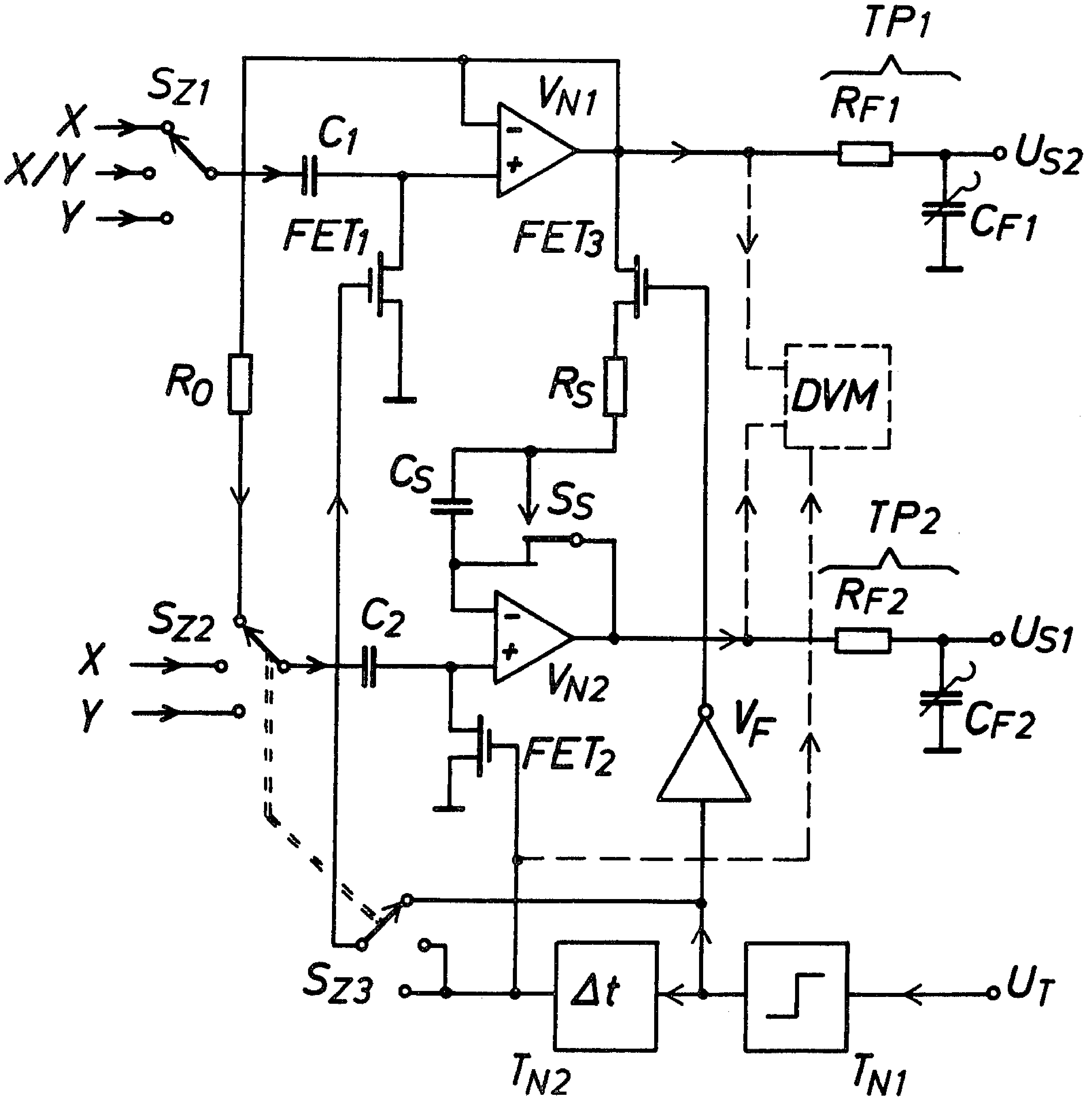

TP1
S_{Z1}
V_{N1}
R_{F1}
X
X/Y
Y
C_1
U_{S2}
FET_1
FET_3
C_{F1}
R_0
R_S
DVM
C_S
S_S
TP2
R_{F2}
S_{Z2}
C_2
X
Y
U_{S1}
V_{N2}
FET_2
V_F
C_{F2}
S_{Z3}
Δt
U_T
T_{N2}
T_{N1}

Fig. 8

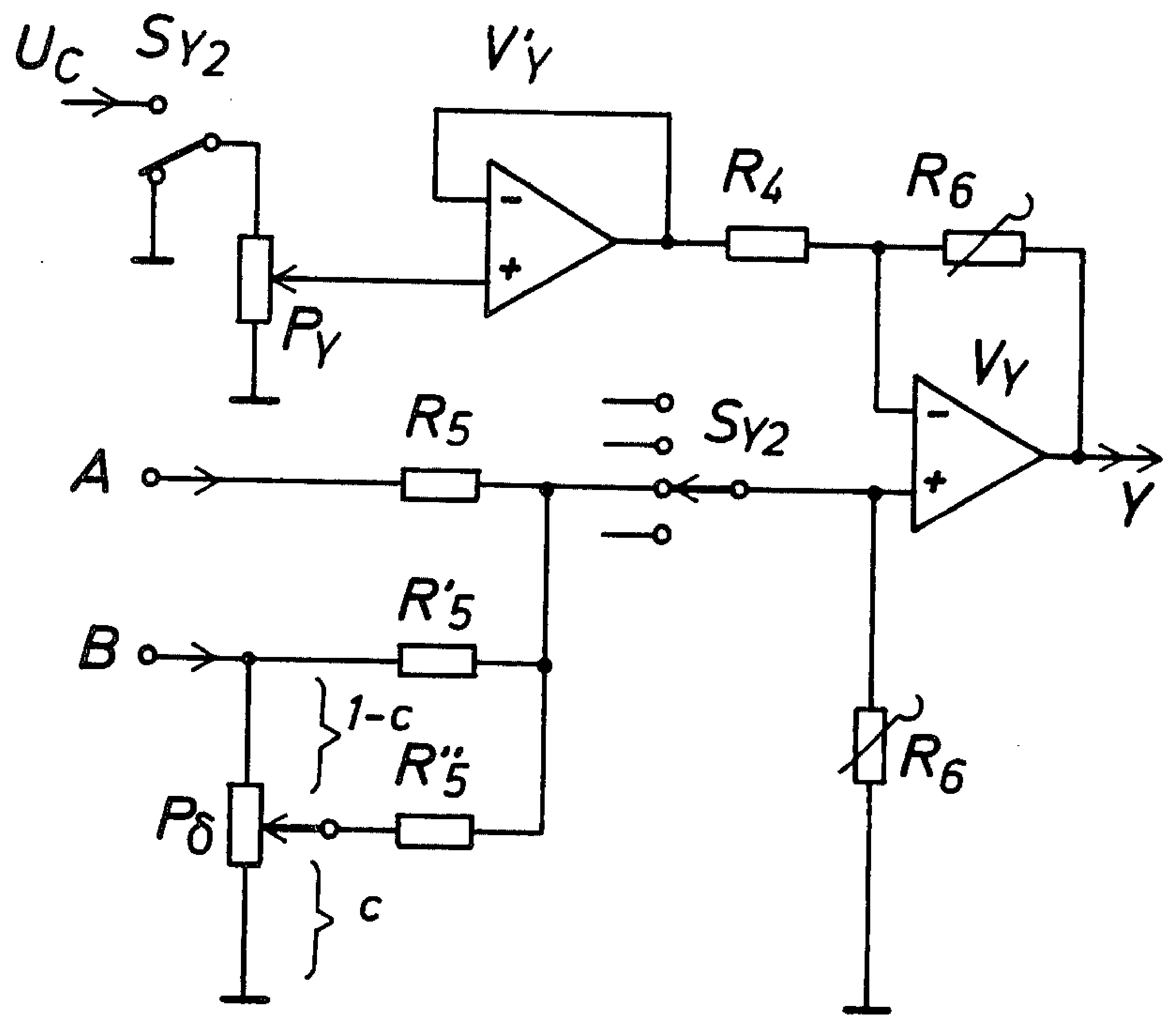
U_C
S_{Y2}
V'_Y
R_4
R_6
P_Y
V_Y
R_5
S_{Y2}
A
Y
B
R'_5
1-c
R''_5
P_δ
c
R_6

Fig. 9

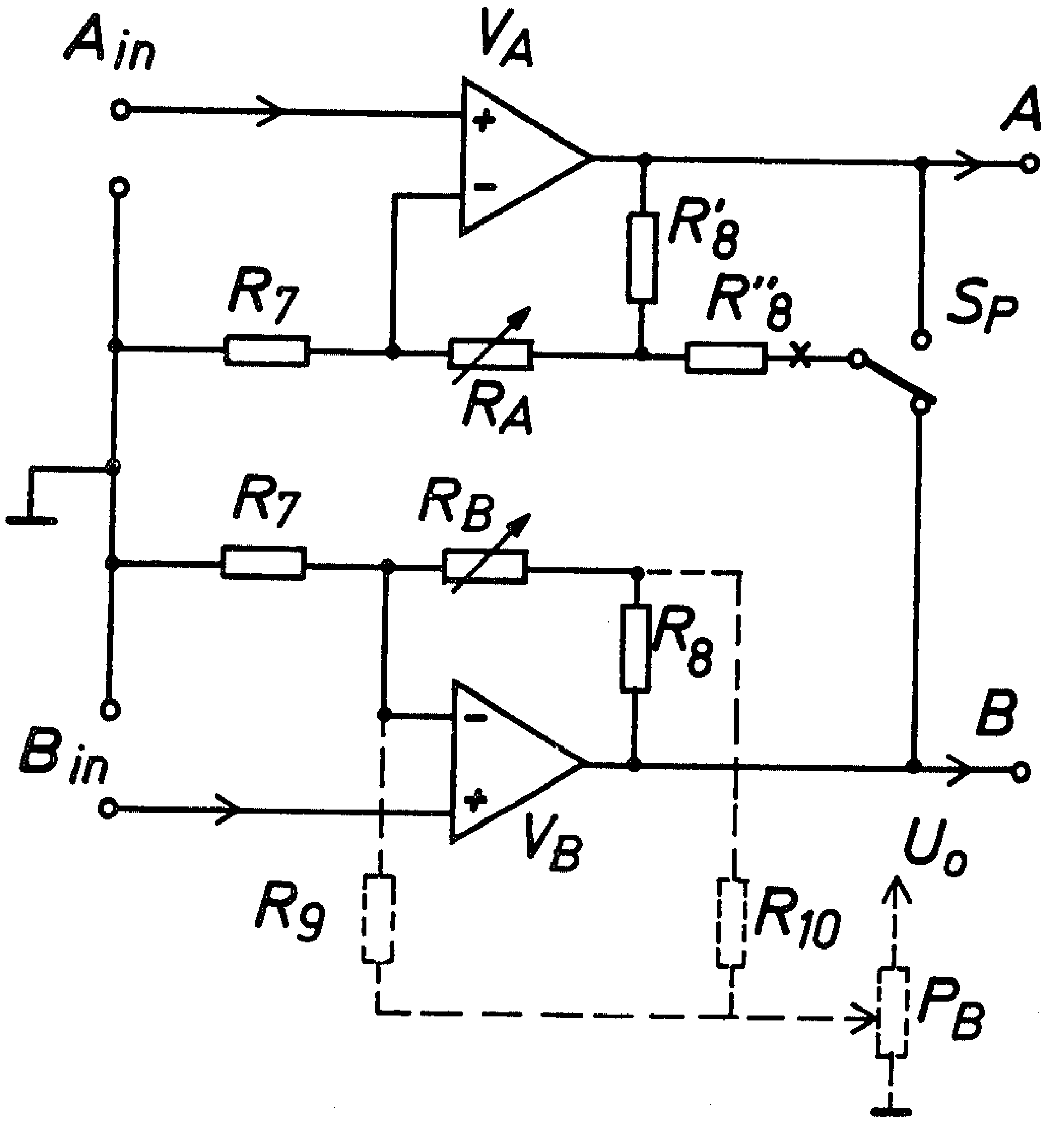
A_{in}
V_A
A
R'_8
R_7
R''_8
S_P
R_A
R_7
R_B
R_8
B
B_{in}
V_B
U_o
R_9
R_{10}
P_B

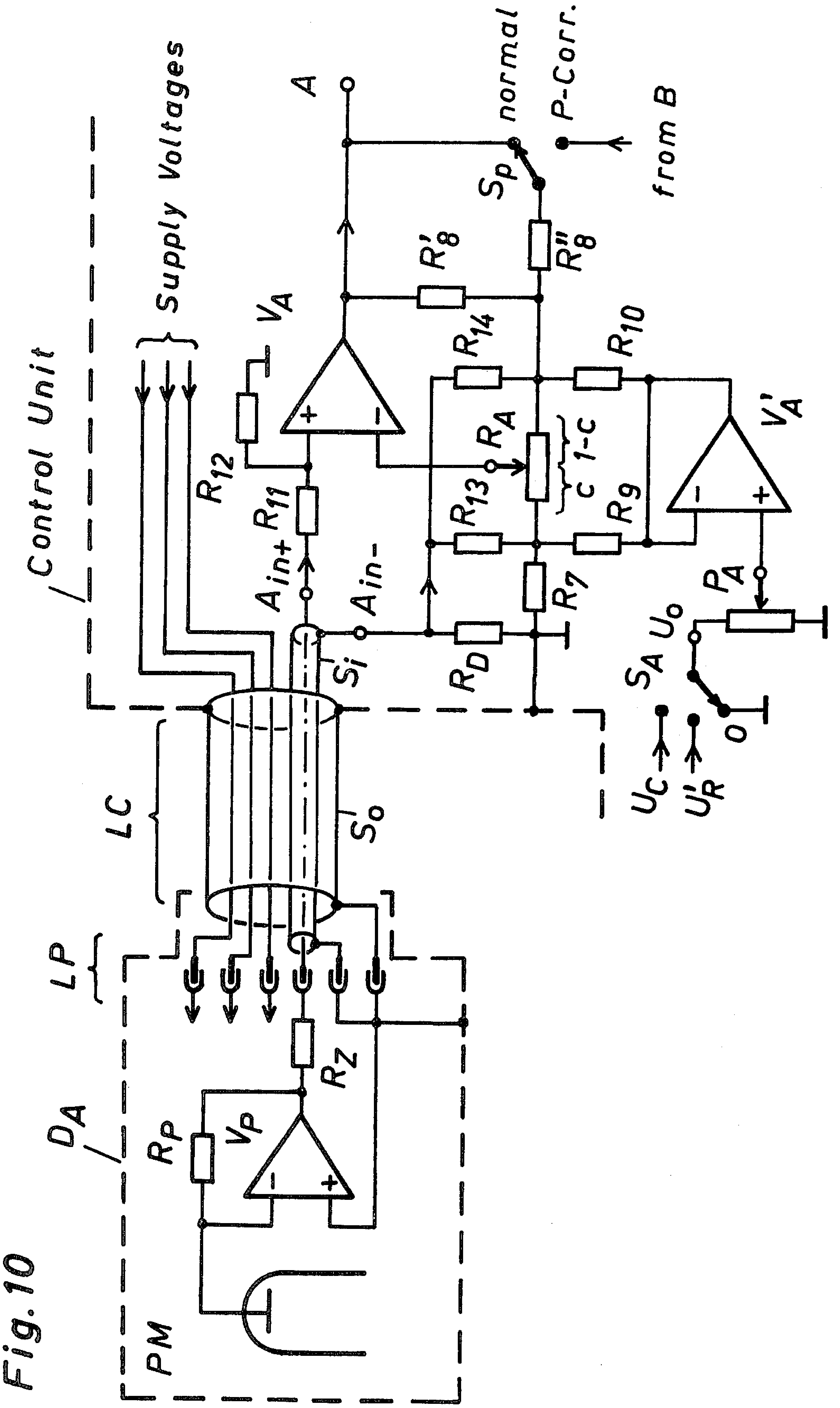
Control Unit
Supply Voltages
A
normal
P-Corr.
from B
S_p
R'_8
R''_8
V_A
R_{14}
R_{10}
R_A
c 1-c
V'_A
R_{12}
R_{11}
R_{13}
R_9
A_{in+}
A_{in-}
R_7
P_A
S_A
U_o
S_i
R_D
0
U_C
U'_R
LC
S_o
LP
R_Z
D_A
R_P
V_P
PM

Fig. 10

APPARATUS FOR INVESTIGATING FAST CHEMICAL REACTIONS BY OPTICAL DETECTION

This is a division, of application Ser. No. 487,592, filed July 11, 1974 now U.S. Pat. No. 3,972,627.

BACKGROUND OF THE INVENTION

The present invention relates to an apparatus for investigating the kinetics of fast chemical reactions in solution using the temperature-jump-relaxation method with spectrophotometric observation of the time course of the reaction with special attention to the fluorimetric technique.

In conventional temperature-jump measurements a sample solution comprising a chemical system under investigation is filled into an optical sample cell having a volume of a few cubic centimeters. The cell is placed in the absorption light path of a spectrophotometer. The equilibrium parameters of the chemical system are changed by a stepwise increase of the temperature ("temperature jump"). Characteristic changes of the absorption spectrum after the temperature-jump indicate how fast the chemical system attains a new equilibrium state and the extent of the concentration changes of the reactants and reaction products. Usually, the temperature-jump is produced by discharging a high-voltage capacitor charge through the electrically conducting sample. To permit such a discharge, the sample cell has two electrodes made of noble metal or stainless steel forming a gap which is perpendicular to the light path. The discharge time and thus the heating time are of the order of one microsecond. The temperature change is several degrees centigrade. (C. F. M. Eigen et al. in: Zeitschr. f. Elektrochemie, Vol. 62, p. 652 (1959), M. Eigen and L. De Maeyer in: Technique of Organic Chemistry, Ed. A. Weissberger, Vol. 8/II, p. 395, Wiley, N.Y. 1963.) Known modifications of the temperature-jump technique use either the cable discharge method or heating by a microwave or infraredlaser pulse.

At low concentrations, and thus low optical absorption, the measurement of the concentration changes by means of absorption becomes difficult. On the other hand, the concentrations cannot be chosen arbitrarily with respect to the equilibrium constant of the chemical system under investigation. If the equilibrium constant of a first order reaction is very large, a temperature-jump experiment only leads to a significant displacement of the equilibrium at low concentrations. This is especially true for many biochemical reactions where the substances involved are active at extremely low concentrations. Furthermore, the costs of material preparation are of importance in biochemical studies. Thus it is of special interest to perform measurements using very small samples and low concentrations. It is also important to improve the specificity of the spectrophotometric detection method.

In the case of static spectrophotometers an improved high sensitivity at low concentrations as well as a high specificity can be achieved by measuring the fluorescence light which is emitted by many organic molecules when excited by light of shorter wavelength, especially ultraviolet light.

Temperature-jump measurements using fluorescence detection involve extremely difficult problems. The signal-to-noise-ratio is proportional to the square root of the light intensity times the signal risetime. The signal risetime of static spectrophotometers is of the order of one second. For microsecond temperature-jump measurements of small differential effects the light intensity should be 10^6 times higher than with static measurements. The most obvious way to obtain a higher light intensity would be to use extremely powerful high-pressure lamps and monochromators. This possibility, however, is limited for chemical reasons, because of the finite photochemical stability of the sample, and for physical reasons, because the highest light intensities cannot be obtained without a decrease in light stability which is also very important for a high-resolution instrument. Due to these difficulties temperature-jump measurements using fluorimetric detection have only been successful in a few cases so far. At low concentrations the signal was lost in the noise.

OBJECTS AND SUMMARY OF THE INVENTION

It is therefore an object of the invention to produce temperature-jump signals of high quality even if small volumes and low concentrations are used. It is further an object of the invention to provide for an apparatus which allows to perform investigations of many different typs with the same sample under reproducable and similar conditions. According to the invention, the sensitivity of a temperature-jump apparatus for fluorimetric measurements is considerably increased by using an immersion lens system in the emission light path. This lens system has an extremely high optical efficiency that exceeds the efficiency of commercial static fluorimeters by orders of magnitude. It is used together with other devices some of which are already known. The high optical efficiency of the measuring arrangement also makes feasible measurements of fluorescence polarization by optional insertion of polarizing elements in the light path. Losses of light cannot be avoided in this case but valuable additional information can be obtained, especially for studying binding of macromolecular substances. The instrument is also adapted for measurements of absorption. Thus comparative measurements of absorption, fluorescence and fluorescence polarization can be performed. Measurements of scattered light at an angle of 90° instead of fluorescence are also possible.

FIG. **1:** Schematic diagram of the optical arrangement of the new apparatus.

FIGS. *2a* to *d:* Vertical cross sections and horizontal cross section of a sample cell Z used in the arrangement according to FIG. **1.**

FIGS. *2e* to *2f:* Horizontal cross sections of modified sample cells.

FIG. **3:** Detailed drawing of the emission light path according to FIG. **1** and arrangement of an immersion lens system of extremely high optical efficiency each of which consists of one spherically ground cell window **5** and one lens L_7 (L_8) mounted in the cell holder HZ.

FIG. **4:** Modified version of the lens system shown in FIG. **3** used to obtain an intermediate image of the sample cell volume.

FIG. **5:** Block diagram of an opto-electronic control unit for processing of the photodetector signals obtained by the arrangement shown in FIG. **1.**

FIG. **6:** Circuit diagram of a zero-correction circuit NA as used in FIG. **5** with optional delayed or nondelayed triggering.

FIG. 7: Circuit diagram of output stage with two zero-correction circuits for independent and cascaded operation.

FIG. 8: Circuit diagram of main amplifier V_Y with correction for the large-aperture error of polarimetric measurements.

FIG. 9: Circuit diagram of input amplifiers V_A and V_B with alternative correction of the large-aperture error.

FIG. 10: Circuit diagram of improved input amplifier V_A and connections between the control unit and photodetector head D_A.

The high-voltage discharge circuit for producing the temperature-jump and the power supply units for the light source, for the discharge circuit, and for the optoelectronic equipment of the apparatus are not shown.

The optical arrangement of the apparatus is shown in FIG. **1.** For a light source Q, high-pressure lamps with mercury and/or xenon filling and a power of 200 watts or more may be used emitting light in the UV and in the visible range. For measurements of absorption in the visible range, a Quartz-iodine-tungsten lamp may also be used. The light is focused onto the entrance slit of a monochromator M by a condensor lens or lens combination L_1. For most applications it is preferable to use a grating monochromator with an aperture ratio of 1:35 or better and a dispersion of 3 nm/mm. The grating is fully illuminated by a field lens L_2. Exposure of the monochromator, the sample and the photodetectors to light can be avoided between measurements by means of a light shutter V.

The monochromator exit slit is imaged onto the sample chamber of the measuring cell Z to form a first light path therethrough by a collimator lens L_3 (e.g. $f = 100$ mm) and a focusing lens L_5 (e.g. $f = 75$ or 100 mm) that provide an image ratio of 1:1 or less. The position of one of these lenses is axially adjustable to correct for the chromatic error of the focusing point. A collecting lens L_6 (e.g. $f = 50$ mm) is used to focus the transmitted light onto the cathode of the absorption photodetector D_o which should have a high cathode current capability (e.g. a photodiode or a side illuminated photomultiplier such as the well known 1P28 of RCA or similar phototubes of other manufacturers). For fluorimetric measurements without simultaneous measurements of absorption the lens L_6 can be replaced by a concave mirror S, thus doubling the light intensity in the sample cell. The fluorescence light emitted from the sample is collected on both sides of the excitation light path in a second light path by means of a lens combination (L_7 or L_8 respectively, together with one spherically ground window on each side of the sample cell Z) and brought onto the photocathodes of the fluorescence photomultipliers D_A and D_B after passing through the filters F_A and F_B. The photocathode of these multipliers should have a high quantum yield in the ultraviolet and the visible range and optimum homogeneity, esp. freedom from orientation effects. The cathode current capability may be lower than for the detector D_o (e.g. 9558Q or 9817Q of EMI or similar with end-on trialkali-cathode, the so-called S-20 UV type). Part of the primary light is brought onto a reference photodetector D_C by means of a beam splitter T, e.g. a thin fused silica plate, and a collecting lens L_4 (e.g. $f = 150$ mm). The reference photodetector D_C should have the same specifications as the absorption photodetector D_o. The fluorescence of highly absorbing samples can also be measured by the front-on technique if the beam splitter T is replaced by a dichroic mirror and the fluorescence photomultiplier D_A and the filter F_A are moved to the left positions (indicated by dotted lines). All the lenses, the beam splitter T and the windows of the sample cell Z are made of high-grade strain-free fused silica (e.g. the material known commercially as Spectrosil).

For measurements of fluorescence polarization a polarizing prism P is inserted in the primary light path on the right-or left-hand side of the collecting lens L_5 (e.g. a Glan-Thompson or a Glan air calcit prism). As analyzers F_A' and F_B' in the emission light path UV-transmitting polarizing foils are preferred (e.g. Kasemann Polarex types KS-W68 and P-UV 2 or Polacoat type UV 105). The mountings of the polarizer P and the analyzers F_A' and F_B' can be rotated. They have stop positions at 0° and 90°, and at 35.° or 54.7° respectively.

All optical elements at the right-hand side of the monochromator can be enclosed in a sample cell compartment to which the photodetectors D_o, D_A, D_B, and D_C are attachted by light-tight flanges.

The temperature-jump cell is shown in FIG. **2.** FIG. *2a* shows a vertical cross section through the axis of the primary or excitation light path, whereas FIG. *2b* shows a vertical cross section through the axis of the secondary or emission light path. FIG. *2c* is a drawing of the horizontal cross section of the cell. FIG. *2d* is an enlarged part of FIG. *2c.* FIGS. *2e* and *2f* demonstrate further modifications.

Besides the maximum yield of the fluorescence light previously mentioned, the design shown in FIG. **2** also fulfills the following requirements:

low intrinsic fluorescence, low stray light and highest possible freedom from strain of the optical elements,

small sample volume,

high ease of operation for concentration series measurements (titrations) without loss of substance.

The body of the sample cell consists of an outer shell of stainless steel **1** and a core **2** made of PTFE ("Teflon"), black polyacetal resin (e.g. "Dynal" or "Delrin") or a similar material. From below it shows the profile of a high voltage insulator **7.** As an alternative the whole cell body can be machined out of one piece of insulating material. The conical cell windows in the excitation light path **3** and in the emission light path **5** have inner diameters of 6 mm e.g., and preferred cone angles, relative to the axis, of 15° and 40°, respectively. They are fixed by mounting rings **4** and **6** which serve also as entrance and exit diaphragms. Special attention has been paid to the different coefficients of thermal expansion. In order to obtain the highest possible freedom from mechanical strain and, at the same time, an optimal tightness the windows are inserted with a solvent-resistant visco-elastic adhesive *2a;* preferably with a polymerizing silicone rubber (shown in FIG. *2d* in an unscaled and rather exaggerated representation). This is in contrast to the earlier manufacturing procedure where the cones had been greased and then pressed into the cell body. For further improvement, the mounting rings **4** and **6** are underlayed by rubber O-rings. The adhesive is dyed black in order to eliminate any light reflections from the conical walls and any fluorescence of the adhesive material. The same or a similar sealing compound is used for insertion of the lower cell electrode **8** to which the high voltage pulse is applied. A plate of noble metal **18** (gold or platinum) has been soldered onto the top of this electrode as the effective material. The upper electrode **9** is grounded and is covered underneath with a cap **19** of the same noble metal. The electrode shaft has been provided with a blind hole **20** for insertion of a temperature sensing probe.

The sample cell is inserted into a cell holder HZ (FIG. **1**) by means of a screw ring or a similar device. Temperature control is done via the cell holder. The cell chamber **13** is square in cross section, e.g. 7 × 7 mm. Consequently, the sample volume of the present construction is approximately 0.7 cm^3. A semi-spherical auxiliary volume **14** is provided above the cell chamber together with a hole **17.** The upper electrode **9** can be removed from the cell by means of a springloaded bayonet socket **10, 11** and **12.** Thus, in contrast to known cell constructions, the cell can be opened for adding substances for titration, without removing the cell itself from the holder. This is especially useful for fluorimetric measurements where only very small additions of substance from a microliter syringe are needed. Known cell constructions with special filling bores do not guarantee such accurate titrations or thorough mixing of the sample solution.

Spherically ground conical cell windows have already been used for a fluorescence temperature-jump apparatus. Additional lenses may be used at the cell windows, but no indication is made about their function, dimensioning, and arrangement (G. Czerlinski, Rev. Sci. Instr. 33, p. 1184 (1962)). For identical cell windows have been used for excitation and emission. This, however, complicates the optimization of the cell with respect to the optical efficiency and, as will be shown below, also with respect to the stray light characteristics.

In contrast to this earlier construction, the sample cell of the new apparatus has a very different dimension in each light path. The free aperture of the excitation windows **3** has been chosen so that the focused light, supplied by a monochromator with a large aperture ratio (e.g. 1:3.5) and by the corresponding optics, can freely pass through the cell without waste of space. A considerably larger conical angle will then be available for the emission windows **5.** Furthermore, the inner diameters of the excitation and the emission windows can exceed 80 percent of the horizontal dimensions of the cell chamber, without loss of mechanical stability. For a given sample volume, the light gathering power of the cell is thus maximized. If a larger sample volume is admitted, the inner diameters of the windows can also be larger, e.g. 8 mm for a sample volume of 2 cm^3, which gives an improved light gathering power.

The unique performance of the new apparatus is obtained by combining the spherically ground emission windows **5** with additional lenses L_7 and L_8 in the cell holder very close to the emission windows. This combination has been calculated as a complete optical system and is shown in detail in FIG. **3.** The radii of curvature of the lens system are, e.g., $\rho_1 = 16.2$ mm for the cell window **5,** and $\rho_2 = 23.4$ mm for the lens L_7 and L_8 (the latter is not shown in FIG. **3**). The distance of the centers of curvature from the center of the cell are $a = 8.8$ mm and $b = 18.0$ mm. With a refractive index of $n = 1.5$ for fused silica and $n = 1.33$ for the solvent (water), the focal point of this immersion lens system lies just in front of the center of the cell. The numerical aperture is approximately 0.75.

The light emitted from the center of the cell passes through the filters F_A and F_A' in slightly convergent, nearly parallel rays. Since the dimensions of the lens system are large compared to the dimensions of the cell chamber, an almost parallel light path is also obtained for light emitted by other volume elements within the cell chamber. The free aperture of the lens L_7 has a diameter of approximately 40 mm that fits the effective cathode diameter of a 2-inch photomultiplier D_A. This adaptation and the nearly parallel light path allow a larger distance between the measuring cell and the photomultiplier, which simplifies the electrical screening. By an appropriate selection of this distance (e.g. 15 cm) the interference of electro-luminescence effects (which sometimes appear during the high-voltage discharge at the cell electrodes) can be avoided, too. In earlier constructions these effects disturbed the fluorescence measurements considerably.

Improved stray light characteristics can be obtained if the lens system in FIG. **3** is modified as shown in FIG. **4** by insertion of a third lens L_7'. The focal length of L_7' should be equal to, or larger than, the focal length of the lens L_7. This triple lens system forms an enlarged image of the cell volume in the space between the lens L_7' and the photocathode. From this image the volume elements of interest are selected by use of one or two diaphragms E_1 and E_2. As an example, stray light emitted from the edges of the excitation and/or the emission windows, can be suppressed. In the arrangement shown in FIG. **4,** the entrance pupil of the left cell window **5'** is imaged on the diaphragm E_1 whereas the entrance pupil of the right cell window **5** is imaged on the diaphragm E_2. Since the image ratio is different in both cases, diaphragms with different apertures are used. The diaphragm E_2 can be omitted if the diameter of the diaphragm required corresponds to the diameter of the photocathode itself. It may be useful to coat the surfaces of the lenses L_7 and L_7' (e.g. for the fluorescence spectral range of 320 to 500 nm which is of special interest for biochemical studies). - Correspondingly to L_7', a lens L_8' with the corresponding diaphragms belongs to the photomultiplier D_B which is not shown in FIG. **4.**

To optimize the spectral efficiency, cut-off filters should be used as emission filters F_A and F_B which cut off the short-wave excitation light and transmit the longer-wave emission light. This is a well known method for obtaining the integral light intensity of the fluorescence emission band. With the new instrument measurements of fluorescence intensities are normally performed with both photomultipliers D_A and D_B in parallel and equal filters F_A and F_B (by using the summing channel Y in FIG. **5**). The signal-to-noise-ratio will thus improve by a factor of $\sqrt{2}$. In emission light paths according to FIG. **3,** the actual improvement has been found to be even higher. Some light which is normally lost by reflexion from the end-on photocathodes is reflected back through the sample cell and contributes to the useful light intensity.

It is also possible to use different filters F_A and F_B in order to separate the emission bands of different chemical species. An optimum light output can be obtained by using dichroic mirrors as wide-band interference filters that reflect the unpassed light back to the opposite channel. The characteristics of non-available passband filters can be simulated by using different cut-off filters F_A and F_B and by forming the difference of the two measuring signals (utilization of the differential channel X in FIG. **5** which is mainly provided for measurements of polarization).

Improved Version of the Sample Cell

It has been found that the stray light characteristics of the sample cell itself are highly dependent on the image quality of the excitation light path in the cell and especially on the form of the excitation windows. A reflection of about 4% occurs at the back of the exit window. (Right-hand window **3** in FIGS. *2a* and *c*. Application of broad-band antireflex coating is difficult in UV.) Part of the reflected light enters the emission windows **5** and thus contributes to the stray light in the emission light path. A similar reflexion occurs at the front of the entrance window if the spherical mirror S is used in FIG. **1**. For lens-ground windows with an unfavourable radius of curvature, as in the case of the above mentioned temperature-jump cell with four identical windows, the stray light is considerable and becomes a limiting factor at low concentrations. Windows which are face-ground on both sides as shown in FIGS. *2a* and *c* have proved to be far less critical in this respect. However, improved stray light characteristics can be obtained by lens-ground windows if the radius of curvature is approximately equal to or slightly larger than the distance from the vertex to the center of the cell. By means of such a spherical lens surface *3a* (in which the focal point almost coincides with the center of the cell) the light is reflected back to the cell chamber with imaging quality, thus contributing to the effective primary light. A cross section of this version is shown in FIG. *2e*. The optimal radius of curvature depends on the thickness of the excitation windows. If the thickness equals two times the distance of the windows, the inner surface of the opposite window should be imaged on itself. If the thickness is very large, the center of the cell should be imaged in itself. A larger thickness than shown in the drawing is recommended, also in case of face-ground excitation windows.

FIG. *2f* shows a sample cell with only three windows which has been designed for simpler apparatus where only one emission detector is used and measurements of fluorescence polarization are not provided. One emission window **5** of FIGS. **2.***b* to *e* is replaced by a cone of fused silica **15** metalized on its spherically ground outside **15***a*. The radius of curvature of the reflecting surface **15***a* should be such that the center of the sample cell is imaged in itself. Instead of a mounting ring **6**, a cover **16** is used. Compared to a three-window cell without the reflector, the reflector improves the light efficiency almost by a factor of 2.5 because the light which is normally lost by the reflectance of the endon photocathode is reflected back to the cathode.

The constructions of windows, sample cells, and lens systems as described in FIGS. **2** to **4** prove to be useful for other apparatus for reaction kinetic measurements which are not discussed here, such as for flow techniques a.o.

Opto-Electronic Control Unit

FIG. **5** shows the block diagram of an opto-electronic control unit corresponding to the optical arrangement shown in FIG. **1**. This control unit is organized as an analog computer and based on operational amplifier techniques (summing and subtracting, continuously and stepwise variable gain factors, electronic division). The circuit shown is provided with two inputs A_{in} and B_{in} which can be connected to two photodetectors in the primary and/or in the secondary light path, e.g. to D_A and D_B. Input C_{in} is connected to the reference detector D_C. For photodetectors photomultiplier circuits with dynode switching are used because of the unconventionally high light intensities in both light paths. For the photodetectors D_o and D_C vacuum or semiconductor photodiodes can be used, too. The photodetectors are incorporated in individual photodetector heads, provided with current-to-voltage converters, and connected to the control unit by multi-lead cables.

Input Amplifiers

Each of the input amplifiers V_A, V_B and V_C has a continuously adjustable gain control for setting a normalized signal A, B and C, respectively. The gain variation may be ×5 **to cover the signal jumps when switching the photodetector dynodes.** Amplifiers V_A and V_B are provided with offset controls P_A and P_B that are normally switched off (potentiometer voltage $U_o = 0$). At low light intensities, these offset controls may be used either for dark current compensation (where U_o is chosen as a constant voltage) or used for stray light compensation (where U_o is proportional to the reference signal C). By applying the compensation voltages directly to the inputs, the amplification of the purified signals A and B can be varied without readjustment of P_A and P_B. The amplifier V_C is provided with an additional RC-lowpass filter TP', with selectable time constants in the microsecond and lower millisecond range, which is used for fast measurements of absorption in order to give lower photon noise of the reference signal. This is especially powerful in comparative measurements of fluorescence and absorption at low sample absorbance. Schematicly drawn as an separate circuit, this lowpass filter is part of the amplifier V_C itself or is followed by a buffer amplifier and does not affect the source impedance at point C.

Main Amplifiers V_X and V_Y and Divider DIV.

Both main amplifiers V_X and V_Y have input selector switches S_{X1} and S_{Y1}, calibrated offset controls P_X and P_Y working on their inputs with switches S_{X2} and S_{Y2}, and selectable gains of, e.g., 1, 2, 5 and 10. The differential amplifier V_X can be switched to give signals A, B, A-B, or B-A. Offset control P_X can be connected to the reference signal C, to the output of amplifier V_Y, or switched off. The summing amplifier V_Y can be switched to give signals A, (A+B)/2, (A/2)+B, or B. Offset control P_Y is connected to C or switched off. In order to obtain the quantity X/Y, both amplifier outputs can be connected to a fast electronic divider DIV (e.g. using transistors in a current-ratioing circuit). The division modes X/C and Y/C are also provided (not shown). By means of a relay, the divider is switched off by a threshold detector T_Y if the denominator becomes too small, e.g. if the light shutter V is closed in FIG. **1**.

Measurements of Fluorescemce Polarization and Organization of Electronically Performed Division

The positions of switches shown in FIG. **5** refer to measurements of the degree of polarization which is defined as

$$p = (I_{\parallel} - I_{\perp})/(I_{\parallel} + I_{\perp}). \qquad (1)$$

$I_{\parallel}$ and $I_{\perp}$ are the intensities of the fluorescence light polarized parallel and perpendicular to the excitation light, respectively. The preferred arrangement of the excitation and of the emission light path in FIG. **1** is in the horizontal plane. Thus the polarizing prism P in the excitation light path is orientated vertically for these measurements. The analyzing filter F_A' is also vertically orientated and the analyzing filter F_B' is horizontally orientated in the emission light path. Thus, $A \sim I_{\parallel}$ and

$B \sim I_\perp$. (Definitions are based on the orientation of the electric field vectors. Filters F_A' and F_B' are set parallel to each other in order to balance the sensitivity of channels A and B.) The control unit is used with $X = A-B$, X-gain $x1$, $Y = (A+B)/2$, and Y-gain $x2$. If the offset switches S_{X2} and S_{Y2} are both grounded, the divider output gives

$$p = (A - B)/(A + B) = X/2Y. \quad (2)$$

For more precise measurements the offset control P_X is switched by S_{X2} to the Y-output and adjusted to compensate for the X signal. The degree of polarization can now be read directly from the offset dial. Changes of the degree of polarization due to a kinetic experiment are obtained as

$$\delta p = p - p_o = [(A-B) - p_o(A+B)/A + B] \quad (3)$$

where p_o is the compensated static value. $X = B-A$ is used if p is negative.

Measurements of polarization based on the fluorescence anisotropy

$$r = (I_{||} - I_\perp)/(I_{||} + 2I_\perp) \quad (4)$$

are very similar except that $Y = (A/2)+B$. This quantity gives the same information as the degree of polarization but it can be more easily handled when evaluating data on a molecular basis.

For optimum sensitivity in measurements of small differential effects, the X-gain is switched to a higher value, e.g. ×5 or ×10, so the complete numerator of eq. (3) is multiplied by a constant factor prior to division. This procedure is mathematically equivalent to a division of $A-B$ by $A+B$ followed by an offset compensation and subsequent amplification. Electronically, however, the described procedure is far superior because the electronic error voltages of the divider, i.e. noise, thermal and temporal instabilities, and static and dynamic errors, have far less influence if the differential signal level is increased first. This is of special interest in kinetic measurements because of the limited accuracy and noise characteristics of fast divider circuits. The same technique is applied, e.g., when measuring fluorescence intensity changes corrected for the inner filter effect (see below).

Measurements of Fluorescence Quantum Yield

Measurements of fluorescence light intensities independent on the orientation of molecules and thus independent of fluorescence polarization must be based on the quantity $I_{||} + 2I_\perp$, where the ratio 1:2 corresponds to the intensity ratio of components $I_{||}$ and $I_\perp$ obtained by integration over the total sphere. $I_{||} + 2I_\perp$ is a measure of the fluorescence quantum field. If the polarizer P and the analyzing filters F_A' and F_B' are in the same position as before, this quantity is obtained by the function $Y = (A/2)+B$. Offset control P_Y is connected to C for measurements of signal changes. The analyzing filters can also be used either in preferred angular positions of 54,7° with respect to the vertical axis, or they can be omitted and the polarizing prism P rotated from the vertical position to an angular position of 35,3°. In both cases, signals A and B can be used separately in channels X and Y, or processed with $Y = (A+B)/2$. Offsets P_X and P_Y are connected to C. Angular stop positions of 53° instead of 54,7° are provided in the emission light path for correction of the large aperture error dealt with below.

Output Stage

The signal obtained at the outputs of the divider and main amplifiers V_X and V_Y can be chosen by a selector switch S_Z and connected to a zero-correction circuit NA that is controlled by an optionally non-delayed or delayed Trigger T_N and followed by a variable RC-low-pass filter TP for optimum filtering of noisy signals. For simultaneous measurements of absorption and fluorescence, or of different fluorescence emission bands in channels A and B connected to V_X and V_Y, two identical output stages are provided one of which is shown in FIG. **5**. The construction of the output stages will be further discussed in FIGS. **6** and **7**.

Meter Circuit and Overload Indicator

For the adjustment and amplitude control of the signals, a digital or analog voltmeter can be switched by a meter selector switch to any point marked by a circle in FIG. **5**: input signals A_{in}, B_{in} and C_{in}, adjusted signals A, B and C, combined signals X and Y, and the divider output X/Y. Measurements of the static signals, especially of A_{in}, B_{in} and C_{in} when performing titrations, have been found to be essential for correct analysis of the kinetic data. On the other hand, setting of normalized adjusted signals A, B and C is much improved by connecting small differential analog meters M_A, M_B and M_C between points A, B and C and a reference voltage where U_R may be either equal to U_C or a fraction thereof or be constant, and $U_{R'}$ is constant. All of the above mentioned signals are controlled by an overload indicator that shows whether any value is out of its proper range. Thus, incorrect settings are easily recognized and nonlinearities are strictly avoided. (Meter selector switch and overload indicator are not shown.)

Extensions

The diagram of the control unit shown in FIG. **5** can be extended by the following components:

a fourth input amplifier for simultaneous connection of all photodetectors shown in FIG. **1**,

additional main amplifiers, similar to the amplifier V_X and V_Y,

additional dividers and especially, additional output circuits NA and TP, for multichannel operation and simultaneous measurements of all spectrophotometric parameters of interest, e.g. absorption, fluorescence intensities, and fluorescence polarization, - or absorption, and fluorescence intensities at different emission wavelengths.

This extension is especially useful for correction of the inner filter effect of fluorescence signals due to the finite absorbance of the sample. It can be shown that in relaxation experiments an appropriate correction can be obtained by dividing the fluorescence signal change by the arithmetic mean of the normalized reference signal C and the normalized signal of the absorption detector D_o. Therefore, one main amplifier should give the sum of both of these signals. The inner filter effect will then be largely suppressed and the quantitative evaluation of signals facilitated.

Another extension deals with digital control and data processing of the apparatus by a digital computer. The outline of the opto-electronic control-unit shown in FIG. **5** is highly suitable for computer controlled operation. The setting of normalized signals A, B and C is especially suited to computer controlled operation. The following additions or modifications have to be made: All signal points marked by a circle in **FIG. 5** (A_{in}, B_{in}, C_{in} etc.) are connected to a multiplexing MOSFET-switch or a similar device and a medium speed digital-to-analog converter for the measurement of static signals prior to each kinetic experiment. For the gain adjustment of the input amplifiers V_A, V_B, and V_C, multiplying digital-to-analog converters are arranged in the feedback loop of these amplifiers. Multiplying digital-to-analog converters can also be used as offset controls P_A, P_B, P_X and P_Y instead of manual potentiometers for balancing of the offset voltages. Semiconductor or relay switches may be used for the selector switches S_{X1}, S_{X2} etc., in the feedback networks of the main amplifiers V_X and V_Y for setting the gain factors, and also in the reference channel for setting the time constant of the lowpass TP'. All of these adjustments need rather slow control operations where a few milliseconds may be sufficient. The digitally set gain factors, offset voltage division factors etc. will be kept by latch-circuits. Further modifications will depend mainly on the available A/D-conversion and data storage system and its capacity. An amplitude resolution of at least 8 bits and a sampling rate of 1 μsec or less are needed for temperature-jump measurements. If the amplitude resolution is 10 bits or more the delayed triggering operation of the zero-correction circuit NA can be omitted, thus simplifying the control-unit. Division and filtering of the output signal can be performed digitally, thus omitting the divider DIV and a digital control circuit for the lowpass TP. Each main amplifier which is connected for measuring a differential signal must have its own zero-correction circuit NA. The divider can also be omitted if an A/D-converter is used without an internal reference voltage and the denominator voltage is applied as the reference source for A/D-conversion.

In order to obtain as much information as possible, the computer controlled version of the apparatus should be provided with the above mentioned fourth input amplifier, additional main amplifiers etc. For alternative manual and computer controlled operation, the most important gain and offsets controls may also be provided for manual operation.

Zero-Correction Circuit NA (FIG. 6)

Basically, this circuit is a high-pass equivalent of a sample-and-hold circuit, modified for the special requirements of relaxation experiments using fluorescence detection. Already described circuits are more complex and/or less versatile for this purpose. The one described in **FIG. 6** consists of a buffer amplifier V_N with a high impedance FET-input (input current e.g. 1 pA), a hold capacitor C_1 with a low leakage current, a resistance R_1 in series with the capacitor, and a resistance R_2 in series with a field effect transistor FET which works as an electronically controlled switch between the amplifier input and ground (e.g. a p-channel enhancement MOS-FET-transistor with an on-resistance $R_F \leqq 150$ ohm). This transistor is normally in the on-state. At the start of the chemical experiment a gate voltage U_T is applied to the trigger T_N. Depending on the trigger delay time Δt, which may be zero or any finite value, the transistor is switched to its off-state either undelayed or delayed. A gate signal coupling transistor T_1, resistors R_3 and R_K, and a small capacitor C_K are provided to produce an electric charge pulse to compensate for a capacitive switching pulse which occurs at the upper electrode of the field-effect transistor due to its gate electrode capacitance (e.g.

$$C_K \simeq 10 \text{ pF}, R_K \simeq R_3/3).$$

If the transistor FET is in its on-state the circuit of **FIG. 6** works as a differentiating circuit with the "settling time constant"

$$\tau_s = C_1 (R_1 + R_2 + R_F). \qquad (5)$$

If the transistor is in its nonconducting off-state the time constant is switched to a very high value (e.g. 10^4 sec) and any signal change that occurs at the input of the circuit is transferred to its output and thus to the lowpass filter TP.

There are three different operational modes depending on the delay time Δt and on the size of the elements C_1, R_1 and R_2. Some typical data are listed in Table I. The delay time Δt may be switched in steps of $1:\sqrt{2}$. C_1, R_1 and R_2 are switched together with the operational modes and with the delay time ranges. If similar circuits are used in other kinetic apparatus designed for longer or shorter time intervalls, the values of Δt and τ_s can be chosen accordingly.

Table I

	Function	Δt_{ms}	$\tau_{s_{ms}}$	$C_{1_{\mu F}}$	$R_{1_{k\Omega}}$	$R_{2_{k\Omega}}$
(1)	Drift-filter	0	5	2.2	0	2.2
	" , simplified	0	1	2.2	0.33	0
(2)	Automatic zero-suppression	0.01.. 0.1	<0.01	0.08	0	0
		0.1.. 1	0.03	0.1	0.15	0
		1 .. 10	0.15	0.33	0.33	0
(3)	Short-circuiting device with drift-filter	0.01.. 0.1	15	2.2	6.8	0

1. Drift-filter ($\Delta t = 0$): Because of the very high sensitivity of the new apparatus, it has been found that exact and temporally constant balancing of the static signals is impossible. Even the smallest thermal and photochemical instability of the sample solution will cause a measurable drift-effect. Frequent and cumbersome rebalancing is avoided by using the zero-correction circuit in its nondelayed drift-filter mode. Prior to measurement the FET is conducting, and drift effects are suppressed by a settling time constant τ_s of the order of 1 ms. As soon as the relaxation experiment has been started the time constant is switched to an extremely high value of up to 10^5 sec which is effectively infinite compared to the fast signal changes due to the chemical processes. The corrected signal starts from an exact zero baseline level. The resistor R_2 blocks noncompensated switching pulse effects at the FET completely and avoids interferences arising from slightly delayed opening of the FET. In simplified circuits the resistor R_2 can be omitted or replaced by a smaller resistor R_1 of, e.g., 330 ohms supposed that the opening delay is of the same order as the lag-time of the input and the main amplifiers and that the switching transients remain small com-

pared to the amplified signals. A finite resistor R_1 then acts as a protection resistor to the FET and to the main amplifier or the divider output. This is appropriate with respect to operating errors. Because of the large size of the capacitor C_1, large charge currents occur if the gate voltage U_T is not applied, especially AC-currents if the photodetectors are exposed to room light.

2. Automatic zero-suppression (preferred range $\Delta t =$ 10 μs..10 ms): Signal drifting prior to measurements is suppressed in a similar way as in the drift-filter mode. The settling time constant τ_s, however, has been chosen to be smaller than the trigger delay time Δt. Thus, fast signal changes occurring during the time Δt are largely suppressed. This is important for measuring slow relaxation effects of small amplitude that follow larger fast effects and have to be displayed on an oscilloscope at full size. Such effects are typical in fluorescence temperature-jump measurements because of the temperature dependence of quantum yields that gives large instantaneous signal changes. The upper limit of τ_s is given by Δt. The lower limit is determined by the optical superimposed on the effective signal. Too small values of τ_s lead to uncontrolled fluctuations of the output signal. The lower limit of C_1 [that also effects τ_s according to eq. **(5)**] is given by the input current of the buffer amplifier V_N and the leakage current of the elements with respect to the size and the time intervall of the measured signal. An optimum performance has been obtained by switching the time constant τ_s together with the delay time Δt where the coupling of τ_s to Δt may be closer than indicated in Table I. At short times Δt the ratio $\tau_s/\Delta t$ must be larger than at longer times. E.g., τ_s may vary by a factor of 30 or 100 if Δt is varied by a factor of 1000. During the delay time the oscilloscope beam is blanked by a voltage U_H supplied by an auxiliary amplifier V_H. A finite value of the resistor R_1 gives a well defined settling time τ_s and reduces precharging of the lowpass filter TP. The maximum value of R_1 is limited with respect to the switching transients of the FET, as above mentioned with the drift-filter. R_1 can be omitted in simplified circuits with less complete suppression of the switching transients. R_1 can also be replaced by a finite R_2 for improving the suppression of switching transients.

3. Short-circuiting device with drift-filter (preferred range $\Delta t =$ 10 μs .. 100 μs): The measuring signal is short-circuited for the set delay time Δt with $R_1 >> R_F$ and $R_2 = 0$. This operational mode is useful in measurements of highest sensitivity in order to suppress electroluminescence effects that sometimes occur in the sample cell during the HV-voltage discharge and depend on the chemical system. This mode of operation avoids precharging of the lowpass filter TP and the irreducible transients then introduced. Contrary to the zero-suppression mode, no zero shift occurs because of the very large settling time $\tau_s >> \Delta t$. Relaxation times shorter than the delay time Δt cannot be detected in this mode but the amplitudes of fast signal changes can still be measured without distortion after delay. During the delay time the oscilloscope beam is blanked as before.

DOUBLED AND CASCADED ZERO-CORRECTION CIRCUITS

FIG. 7 shows a doubled output stage with two zero-correction circuits and two low-pass filters TP **1** and TP **2** that can be used either for simultaneous measurements of two of the three signals X, Y, and X/Y, as mentioned before, or cascaded for nondelayed and delayed measurements of the same signal. The time constants of TP **1** and TP **2**, given by the elements R_{F1}, C_{F1}, R_{F2} and C_{F2}, can be set independently for optimum matching to the measuring time intervalls. Two buffer amplifiers V_{N1}, V_{N2}, hold capacitors C_1, C_2 (both selected according to Table I), and field-effect transistors FET **1**, FET **2** are provided. Resistors R_1, R_2, R_3 and R_K and transistors T_1 are not shown in this diagram and shall be chosen as FIG. **6.** Two triggers T_{N1} and T_{N2} are series- or parallel-connected to the gate voltage U_T. T_{N1} is nondelayed operated only whereas T_{N2} corresponds to the trigger T_N in FIG. **6.** The measuring signals are selected by switches S_{Z1} and S_{Z2}. The control voltage of FET **1** can be selected by a switch S_{Z3} coupled to S_{Z2}. In the upper position of S_{Z2} and S_{Z3} both zero-correction circuits are cascaded to obtain nondelayed and delayed output signals U_{S1} and U_{S2}. With respect to the output current capability of V_{N1} a decoupling resistor R_o of, e.g., 200 ohms can be provided between V_{N1} and S_{Z2}.

In many cases where recording the delayed signal U_{S2} is insufficient, however, it is adequate to measure the time course of U_{S2} together with the voltage shift $\Delta U_S = U_{S1} - U_{S2}$ instead of both voltages U_{S1} and U_{S2}. The voltage ΔU_S is kept in the capacitor C_2 during measurement. It can be measured by a digital voltmeter DVM connected to the output of the two amplifiers V_{N1} and V_{N2} and controlled by the trigger T_{N2} (in FIG. **7** drawn in broken lines). The voltmeter therefore must have a differential input, controlled start and hold and an adequate A/D-conversion time. The trigger T_{N1} should be provided with a gate pulse prolongation circuit if the voltage U_T can be applied for a shorter time than needed for A/D-conversion (e.g. 100 ms).

In the circuit shown in FIG. **7** any voltmeter can be used for measuring the voltage ΔU_S instead of the described one if a special storage capacitor C_S is connected between the amplifier outputs by a decoupling resistor R_S and a field-effect transistor FET **3** which is controlled by an inverting amplifier V_F and is conducting during measurements only. After measurement, a push-botton or a relay contact S_S is switched to its upper position and the voltage ΔU_S is obtained between the output of V_{N2} and ground. Contrary to the value of C_2 in the delayed mode, the capacitance of C_S may be a few microfarads so that ΔU_S is stored for even longer times without error. The charge time constant, given by C_S, R_S and the on-resistance of FET **3**, may be of the order of 10 ms.

Large-Aperture Correction Circuit for Measurements of Fluorescence Polarization

The large aperture of the sample cell Z shown in FIG. **2** results in a depolarization of the emitted fluorescence light. The effective half-aperture angles, relative to the axis and to the refractive index of water, are approximately 8° with the excitation light path and 34° with the emission light path. With the polarizing prism P in the vertical position and analyzing filters F_A' and F_B' in the vertical and horizontal positions, respectively, the normalized signals A and B are not equal to $I_{||}$ and $I_{\perp}$, as assumed in eq. **(1)**, but

$$A = (1 - \delta)I_{||} + \delta.I_{\perp}$$

$$B = \delta'.I_{||} + (1 - \delta')I_{\perp}. \qquad (6)$$

With the above apertures angles, $\delta = 8\%$ and $\delta' = 0.5\%$. Thus, the measurement of the emission component $I_{\parallel}$ is affected mainly whereas B is still almost equal to $I_{\perp}$. If the aperture error is neglected, an apparent degree of polarization p' is measured instead of the true degree of polarization p:

$$p' = \frac{A - B}{A + B} = \frac{(1 - \delta)I_{\parallel} - (1 - \delta)\, I_1}{(1 - \delta)I_{\parallel} - (1 + \delta)I_1} = \frac{(1 - \delta)p}{1 - \delta \cdot p} \qquad (7)$$

where, as an approximate, the contribution of δ' is omitted. In order to avoid numerical conversion of the measured data an electronic correction is applied, two versions of which are described in FIGS. **8** and **9.**

In FIG. **8** a special coefficient network is used at the input of the main amplifier V_Y. An adjustable correction for measurements with cells of different aperture is provided by a correction potentiometer Pδ. With the selector switch S_{Y1}, only the connection corresponding to the function $y = (A+B)/2$ is shown (slider of P_δ in the upper position). Summing resistors are R_5, R_5' and R_5'' where

$$1/R_5 = 1/R_5' + 1/R_5', \qquad (8)$$

e.g. $R_5'' = 5R_5$, and the resistance of P_δ is small compared to R_5'', c is the voltage division factor of P_δ. P_δ is calibrated in terms of

$$\delta = (1-c)R_5/2R_5'' \qquad (9)$$

in order to give the function

$$y = [A + (1-2\delta)B]/2 \qquad (10)$$

Resistors $R_4 = R_5/2$ and R_6 are used in the feedback loop of the amplifier V_Y for setting the Y-gain as usual. The offset circuit with switch S_{Y2}, offset control P_Y and a buffer amplifier V_Y' is switched off. Thus, if the Y-gain is $x2$, the degree of polarization is measured as

$$p = \frac{A - B}{A + (1 - 2\delta)B} = \frac{(1 - \delta)\,(I_{\parallel} - I_1)}{(1 - \delta)\,(I_{\parallel} - I_1)} \qquad (11)$$

A more complete correction including the coefficient δ' in eq. (6) can be obtained by providing a slightly reduced gain with the A-input of amplifier V_Y which can also be made adjustable. This modification is useful if the large aperture error of the sample cell is added to the error due to an incomplete polarization of the analyzing filters F_A' and F_B' which can be corrected by the same circuit.

According to FIG. **9** the correction of the large aperture error can also be performed at the input amplifiers V_A and V_B. This is especially useful for correcting alternative measurements of the degree of polarization, of the polarization anisotropy eq. (4), and of the fluorescence quantum yield $I_{\parallel} + 2I_{\perp}$. In the circuit shown in FIG. **9**, the error component $\delta.I_{\perp}$ is eliminated by subtracting part of the adjusted signal B from the signal A and then increasing the amplification of the remaining signal $(1-\delta)I_{\parallel}$ by a factor of $1/(1-\delta)$. Both input amplifiers V_A and V_B have feedback networks with variable resistances R_A and R_B for gain adjustment, and fixed resistors R_7, R_8, R_8' and R_8'' where

$$1/R_8 = 1/R_8' + 1/R_8'' \qquad (12)$$

and

$$\delta = R_8/R_8'' \qquad (13)$$

if the switch S_P is in its normal upper position, the gain of the amplifier V_A is

$$v = (R_7 + R_8 + R_A)/R_8 \qquad (14)$$

In the lower position of S_P, the output signal is

$$A_{corr} = A_{in} \cdot v \cdot R_8'/R_8 - B \cdot R_8'/R_8'' = \frac{v}{1 - \delta} A_{in} - \frac{\delta}{1 - \delta} B_{in} \qquad (15)$$

where $v.A_{in}$ is the uncorrected signal A. The gain of amplifier V_B is given by eq. (14) when substituting R_A by R_B. Values are, e.g., $\delta = 0.08$, $R_8 = 820\ \Omega$, $R_8' = 891\ \Omega$, $R_8'' = 10.3\ k\Omega$, $R_4 = 1.6\ k\Omega$ and R_A and $R_B = 0..10\ k\Omega$ for $v = 1.5..7.5$. The gain of both input amplifiers has to be adjusted with equally orientated analyzers F_A' and F_B' to the same normalized values A and B as before. For adjustment of signal A, the switch S_P must not be set back to its upper position if signal B is adjusted prior to A. Thus, the circuit shown in FIG. **9** can be easily operated.

Improvements

In FIG. **9** a continuous setting of the large aperture correction similar to FIG. **8** can be obtained by connecting a potentiometer between the output of amplifier V_A and the commutating contact of switch S_P and connecting the resistor R_8'' to the slider of the potentiometer (modifications at the point marked by a cross in FIG. **9**). In this case eq. (13) applies to the maximum value of δ. E.g., $R_8' = 902\ \Omega$ and $R_8'' = 8{,}2\ k\Omega$ for $\delta = 0..0.10$. For a linear calibration, the potentiometer has to have a low impedance compared to R_8'', or it can be followed by a buffer amplifier. — A correction of the smaller error coefficient δ' in eq. (6) can be obtained by providing a similar circuit with the feedback network of input amplifier B.

Input Offset Circuit

Elements R_9, R_{10} and P_B (in FIG. **9** drawn in broken lines with the input amplifier B) show how the above mentioned input offset voltage can be introduced without interference to the gain adjustment procedure. Therefore, the bridge condition is

$$R_9/R_7 = R_{10}/R_8. \qquad (16)$$

A buffer amplifier can be inserted at the slider of the offset potentiometer P_B in order to obtain a linear calibration. The gain formula (14) becomes slightly modified but eqs. (12) and (13) are not modified.

Screening Problems

Electrical screening between the opto-electronic detection system and the high-voltage discharge circuit is most important in temperature-jump-experiments. When discharging the high-voltage capacitor, the slew rate of the voltage across the sample cell is $dU/dt \simeq 10^{12}$ V/s, and that of the current is $dI/dt \simeq 10^{10}$A/s. A damping factor $\leqq 160$ dB at the opto-electronic system is needed to avoid interferences. This value cannot be safely obtained by conventional shielding. A coaxial design of the discharge circuit is already known. Improved shielding can be obtained by a very compact design of the opto-electronic system. This, however, contradicts the above mentioned arrangement of the photodetectors in individual photodetector heads which is needed for optimal flexibility of the optical design, e.g. for moving the photodector D_A to its left position in FIG. **1**. For measurements of fluorescence polarization, it is also important to have the end-on photodetectors D_A and D_B in-line arranged with the emission light path. This results in relatively long cables between the detector heads and the control unit.

Improved suppression of interfering electrical effects has been obtained by the arrangement shown in FIG. **10** that is outlined for the detector head D_A and the input amplifier V_A which is provided with a differential input circuit. On the left side of FIG. **10**, part of the photodetector tube PM, a load resistor R_P and an operational amplifier V_P connected as a current-to-voltage converter are shown. The detector head is connected to the control unit by a multi-lead connector LP and a multi-lead cable LC which contains the supply voltage leads and a smaller coaxial cable for the signal voltage connection. Thus, a double screening is obtained. The outer screen L_o connects the casings of the detector head and of the control unit directly. The inner screen L_i connects the differential input A_{in-} to the detector head ground whereas the inner coaxial conductor connects the other differential input A_{in+} to the signal output of the detector head. The resistor R_Z matches the detector head to the characteristic impedance of the coaxial cable of, e.g., 50 or 75 δ. At the control unit input A_{in-} a damping resistor R_D of, e.g., 15 δ is provided which can also be series-connected with a capacitor of, e.g., 0.1 μF. Both resistors R_Z and R_D have been found to be useful for damping spurius RF-pick-up produced by the high-voltage discharge, which otherwise could affect the input of the amplifier V_A even if the RF-frequency is too high to be transferred to the control unit output. For frequencies within the passband of the control unit the differential input is matched by small capacitors parallel to the resistor R_{12} and with the feedback network of amplifier V_A (not shown in FIG. **10**). Thus, a common-mode suppression of 50 dB is obtained for most of the frequency range which adds to the suppression obtained by proper electric shielding.

Various differential amplifier circuits can be used for this purpose. The one shown at the right side of FIG. **10** is a differential version of the non-differential amplifier circuit of FIG. **9**. It combines the unique feature of the large aperture correction and the application of the input offset voltage already described with a differential amplifier that needs only one adjustable element with one arm for continuous gain adjustment. Especially, only one high precision amplifier V_A is needed, compared to two of these amplifiers in more conventional circuits. Amplifier V_A' is provided as an offset-generator only and may be a low cost type. Together with eqs. (12) and (13) for the large aperture correction, where $1/R_8 = 1/R_3' + 1/R_8''$, and eq. (16) for the offset circuit, there are the following bridge circuit conditions for correct differential operation:

$$R_7/R_8 = R_9/R_{10} = R_{13}/R_{14} \qquad (17)$$

and

$$(R_{11} + R_Z)/R_{12} = R_{13}(1/R_7 + 1/R_9) \qquad (18)$$

For improved gain adjustment the variable resistor R_A of FIG. **9** has been replaced by a potentiometer R_A, where c is the voltage division factor. The gain of the input amplifier circuit is then

$$v = \frac{R^*}{R_{13}} \cdot \frac{R^* + R_A}{R^* + cR_A} \cdot \frac{R_8 + R^{**}}{R^{**}} \qquad (19)$$

where

$$1/R^* = 1/R_7 + 1/R_9 + 1/R_{13} \qquad (20)$$

and

$$1/R^{**} = 1/(R^* + R_A) + 1/R_{10} + 1/R_{14} \qquad (21)$$

The gain relative to the voltage at the slider of the offset potentiometer P_A is

$$V' = (R_{13}/R_9).v \qquad (22)$$

For practical reasons one may set $R_7 = R_8 = R_{13} = R_{14}$ and $R_9 = R_{10} = 5R_7$, e.g. $R_7 = 1.5$ kΩ. With $R_Z = 50$ Ω and $R_{11} = 1.5$ kΩ, one has $R_{12} = 1.292$ kΩ. For $\delta = 0.083$: $R_8' = 1.636$ kΩ and $R_8'' = 18$kΩ. A low inductance 10-turn potentiometer of 2 kΩ can be used for R_A which gives $v = 1.25$ .. 5 and $v' = 0.25$.. *1.*

The design of the input amplifier V_B is identical to V_A except that the resistor R_8' is replaced by R_8 and that the switch S_P and the resistor R_8'' are omitted. (For modifications, such as continuous adjustable corrections of coefficients δ and δ', see above.) Both amplifiers have offset switches such as S_A with P_A for selecting for U_o either U_C, or a constant voltage U_R' or zero. Input amplifier V_C has a differential input, too, and the above mentioned lowpass filter TP', but no offset generator. The connections to the photodetector heads are the same as in FIG. **10**. Induced error voltages are largely avoided by the multi-lead cables.

What is claimed is:

1. In an apparatus for investigating the course of fast chemical reactions by optical detection, said reactions being initiated in a chemical system by an external perturbation using a high-voltage pulse, said apparatus comprising a sample cell holding a liquid sample of said chemical system, means performing said perturbation, monochromatic illumination means, a reference beam divider, at least one light path transversing said sample cell, and optical detection means including at least two photodetectors operatively connected to a signal processing unit provided with individual input amplifiers, the improvement wherein said photodetectors are arranged as individual photodetector heads in operative position, said photodetector heads comprising photomultiplier tube, dynode switching network, current-to-voltage transducer and housing and shielding means, said input amplifiers having differential input, each of said photodetector heads being connected to said signal processing unit by a shielded multi-lead cable and multi-lead connector, said cable comprising an inner shielded signal cable connected to said differential input, further comprising supply leads for operating said photomultiplier tube and said current-to-voltage transducer, and also respective photodetector head to the housing of said signal processing unit.

2. Apparatus according to claim **1**, wherein said input amplifiers have variable gains, each input amplifier circuit comprising: first and second input terminal, one variable attenuator, first, second and third fixed voltage divider having upper and lower ends and one tap each, one operational amplifier having noninverting and inverting input, and output; wherein: said first fixed divider has connected its upper end to said first terminal, its tap to said non-inverting input, and its lower end to signal grounding potential, said second and third fixed divider have connected their upper ends to said second terminal, their taps to one end each of said variable attentuator, and their lower ends to signal grounding potential and said output, respectively, said inverting input being connected to said variable attenuator, said fixed dividers having equal division factors with respect to source voltages at said input terminals.

3. Apparatus according to claim **2** wherein said second and third fixed divider have auxiliary inputs connected to a variable offset source, giving equal division factors at said variable attenuator.

* * * * *